Supplementary data for article:

Filipović, N. R.; Elshaflu, H.; Grubišić, S.; Jovanović, L. S.; Rodić, M.; Novaković, I.; Malešević, A.; Djordjević, I. S.; Li, H.; Šojić, N.; et al. Co(III) Complexes of (1,3-Selenazol-2-Yl)Hydrazones and Their Sulphur Analogues. *Dalton Transactions* **2017**, *46* (9), 2910–2924. https://doi.org/10.1039/c6dt04785h

Electronic Supplementary Information

Co(III) Complexes of (1,3-Selenazol-2-yl)hydrazones and Their Sulphur Analogues: Comparative Structural, Electrochemical, Computational and Biological Activity Study

Nenad R. Filipović[a], Hana Elshaflu[b], Sonja Grubišić[c], Ljiljana S. Jovanović[d], Marko Rodić[d], Irena Novaković[c], Aleksandar Marinković[b], Aleksandar Mališević[e], Ivana S. Djordjević[c], Haidong Li[f], Nešo Šojić[f], Tamara R. Todorović[e,*]

[a]*Department of Chemistry and Biochemistry, Faculty of Agriculture, University of Belgrade, Nemanjina 6, Belgrade, Serbia;* [b]*Faculty of Technology and Metallurgy, University of Belgrade, Karnegijeva 4, Belgrade, Serbia;* [c]*Institute of Chemistry, Technology and Metallurgy, University of Belgrade, Njegoševa 12, Belgrade, Serbia;* [d]*Department of Chemistry, Faculty of Sciences, University of Novi Sad, Trg Dositeja Obradovića 4, Novi Sad, Serbia;* [e]*Faculty of Chemistry, University of Belgrade, Studentski trg 12–16, Belgrade, Serbia;* [f]*University of Bordeaux, Bordeaux INP, ENSCBP, Institut des Sciences Moléculaires, CNRS UMR 5255, 16 Avenue Pey-Berland, 33607 Pessac, France.*

[*]Corresponding author:
dr Tamara R. Todorović, Assistant Professor
Faculty of Chemistry - University of Belgrade
Studentski trg 12–16
11000 Belgrade, Serbia
Tel: +381 11 3336731
E-mail: tamarat@chem.bg.ac.rs

Contents

EXPERIMENTAL

Materials and methods

Thiosemicarbazide (99 %), potassium selenocyanate (99 %), hydrazine hydrate (99 %), 2-formylpyridine (99 %) and 2-bromoacetophenone (98 %) were obtained from Acros Organics. 2-Bromo-1-(4-methoxyphenyl)ethan-1-one (97 %) and 2-bromo-1-(4-methylphenyl)ethan-1-one (97 %) were obtained from Maybridge. Cobalt(II) tetrafluoroborate hexahydrate (99 %) was obtained from Aldrich (Sigma-Aldrich Chemie GmbH, Steinheim, Germany). All solvents (reagent grade) were obtained from commercial suppliers and used without further purification.

Elemental analyses (C, H, N, S) were performed by the standard micromethods using the ELEMENTAR Vario EL III CHNS/O analyzer. Infra-red (IR) spectra were recorded on a Thermo Scientific Nicolet 6700 FT-IR spectrometer by the Attenuated Total Reflection (ATR) technique in the region 4000−400 cm^{-1}.Abbreviations used for IR spectra: vs, very strong; s, strong; m, medium; w, weak. The NMR spectra were performed on a Bruker Avance 500 equipped with broad-band direct probe. NMR spectral assignments and structural parameters were obtained by combined use of 1H homonuclear spectroscopy (2D COSY) and multinuclear proton detected spectroscopy (2D HSQC, 2D HMBC). Chemical shifts are given on δ scale relative to tetramethylsilane (TMS) as internal standard for ^{1}H and ^{13}C. Abbreviations used for NMR spectra: s, singlet; dd, doublet of doublets; ddd, double double doublet. UV-Vis spectrum was recorded on Uv-1800 Shimadzu spectrophotometer in 250–600 nm range using a quartz cell with 1.0 cm path length. For 2,2-diphenyl-1-picrylhydrazyl (DPPH) scavenging activity, absorbance at 517 nm was measured using a Thermo Scientific Appliskan. Molar conductivity measurement was performed at ambient temperature on the Crison Multimeter MM41.

Synthesis of compounds

Acetone selenosemicarbazone was prepared by literature procedure.[S1] Hydrazine hydrate was added into the solution of KSeCN in minimal amount of water, followed by dropwise addition of 3.8 N HCl. Acetone was added into the reaction mixture, heated for 1 h, cooled and precipitated acetone selenosemicarbazone separated by filtration.

Selenosemicarbazide was obtained from reaction of acetone selenosemicarbazone with hydrazine in methanol.[S2] Resulting colorless crystals, separated on cooling, were recrystalized from 80 % ethanol, dried in dessicator and stored in dark.

2-Formylpyridine selenosemicarbazone (Hfpsesc) and 2-formylpyridine thiosemicarbazone (Hfptsc) were obtained by condensation of 2-formylpyridine with selenosemicarbazide/thiosemicarbazide according to the reported literature procedures.[S3,S4]

General procedure for synthesis of HL(Se/S)$^{1-3}$·HBr. Example HLSe^{1}·HBr: 2-Bromoacetophenone (0.10 g; 0.5 mmol) was added into suspension of Hfpsesc (0.11 g; 0.5 mmol) in 20 mL of absolute EtOH and stirred for 3 h at room temperature. Red precipitate was filtered off and washed three times with EtOH. Yield: 0.15 g (74 %). Anal. Calcd for $C_{15}H_{13}BrN_4Se$ (%): C, 44.14; H, 3.21; N, 13.73. Found: C, 44.28; H, 3.28; N, 13.69. Λ_M (1×10^{-3} M, MeOH) = 99.1 Ω^{-1} cm^2 mol^{-1}.

Synthesis of HLSe^{1}: 2-Bromoacetophenone (0.10 g; 0.5 mmol) was added into suspension of Hfpsesc (0.11 g; 0.5 mmol) in 20 mL H_2O / EtOH mixture (1 : 1, v/v) and stirred for 3 h at room temperature. Yellow precipitate was filtered off and washed three times with H_2O and EtOH. Yield: 0.11 g (68 %). Anal. Calcd for $C_{15}H_{12}N_4Se$ (%): C, 55.05; H, 3.70; N, 17.12. Found: C, 55.23; H, 3.82; N, 17.29. IR (ATR, ν_{max}/cm^{-1}): 3054 (w), 2958 (w), 2847 (w), 2714 (m), 1596 (m), 1570 (s), 1480 (s), 1434 (m), 1355 (m), 1261 (s), 1144 (s), 1027 (w), 1001 (w), 923 (w), 893 (w), 766 (m), 700 (s), 656 (w), 591 (w), 515 (w). ^{1}H NMR (500.26 MHz, DMSO-d6) δH: 7.30 (t, 1H, J = 7.2 Hz), 7.36 (m, 1H), 7.40 (t, 2H, J = 7.6 Hz), 7.76(s, 1H), 7.87 (m, 4H), 8.12 (s, 1H), 8.58 (d, 1H, J = 4.4 Hz), 12.54 (s, 1H). ^{13}C NMR (126.0 MHz, DMSO-d6) δC: 108.17, 119.20, 123.70, 125.77, 127.40, 128.60, 135.37, 136.79, 142.26, 149.47, 151.45, 153.16, 170.99.

Synthesis of HLSe^{2}: HLSe^{2} was synthesized in a similar way to **HLSe^{1}**, but using 2-bromo-4'-methoxyacetophenone (0.11 g; 0.5 mmol) instead of 2-bromoacetophenone. Yield: 0.13 g (72 %). Anal. Calcd for $C_{16}H_{14}N_4OSe$ (%): C, 53.79; H, 3.95; N, 15.68. Found: C, 53.48; H, 4.12; N, 15.32. IR (ATR, ν_{max}/cm^{-1}): 2929 (w), 2832 (w), 2677 (m), 1598 (m), 1574 (s), 1482 (s), 1249 (s), 1028 (m), 843 (w), 666 (w). ^{1}H NMR (500.26 MHz, DMSO-d6) δH: 3.78 (s, 3H), 6.95 (d, 2H, J = 7.0 Hz), 7.37 (m, 1H), 7.56 (s, 1H), 7.78 (d, 2H, J = 8.8 Hz), 7.86 (m, 2H), 8.11 (s, 1H),

8.58 (d, 1H, *J* = 4.7 Hz), 12.49 (s, 1H). ^{13}C NMR (126.0 MHz, DMSO-d6) *δ*C: 55.10, 105.64, 113.95, 119.19, 123.66, 127.08, 128.60, 136.79, 142.20, 149.45, 153.19, 158.68, 170.94.

Synthesis of HLSe^{3}: HLSe^{3} was synthesized in a similar way to **HSe^{1}**, but using 2-bromo-4'-methylacetophenone (0.11 g; 0.5 mmol) instead of 2-bromoacetophenone. Yield: 0.12 g (69 %). Anal. Calcd for $C_{16}H_{14}N_4Se$ (%): C, 56.31; H, 4.13; N, 16.42. Found: C, 55.99; H, 3.96; N, 16.45. IR (ATR, ν_{max}/cm^{-1}): 2970 (w), 2953 (w), 2711 (w), 1601 (m), 1573 (s), 1481 (s), 1433 (m), 1257 (m), 1148 (m), 1039 (w), 818 (w), 667 (w). ^{1}H NMR (500.26 MHz, DMSO-d6) *δ*H: 2.30 (s, 3H), 7.19 (d, 2H, *J* = 8.0 Hz), 7.35 (m, 1H), 7.66 (s, 1H), 7.73 (d, 2H, *J* = 8.1 Hz), 7.84 (m, 1H), 7.86 (m, 1H), 8.11 (s, 1H), 8.57 (d, 1H, *J* = 4.7 Hz), 12.54 (s, 1H). ^{13}C NMR (126.0 MHz, DMSO-d6) *δ*C: 20.79, 106.94, 119.20, 123.68, 125.71, 129.17, 132.65, 136.67, 136.80, 142.21, 149.45, 151.67, 153.18, 170.97.

Synthesis of HLS^{1}: 2-Bromoacetophenone (0.10 g; 0.5 mmol) was added into suspension of Hfptsc (0.09 g; 0.5 mmol) in 20 mL H_2O / EtOH mixture (1 : 1, v/v) and stirred for 3 h at room temperature. Yellow precipitate was filtered off and washed three times with H_2O and EtOH. Yield: 0.11 g (76 %). Anal. Calcd for $C_{15}H_{12}N_4S$ (%): C, 64.26; H, 4.31; N, 19.98; S, 11.44. Found: C, 63.98; H, 4.09; N, 20.17; S, 11.39. IR (ATR, ν_{max}/cm^{-1}): 3053 (w), 2953 (w), 2747 (w), 1696 (m), 1570 (s), 1481 (m), 1435 (w), 1262 (m), 1144 (m), 767 (m), 700 (m). ^{1}H NMR (500.26 MHz, DMSO-d6) *δ*H: 7.30 (t, 1H, *J* = 7.3 Hz) 7.34 (m, 1H), 7.35 (s, 1H), 7.40 (t, 2H, *J* = 7.7 Hz), 7.85 (m, 4H), 8.08 (s, 1H,), 8.57 (d, 1H, *J* = 4.4 Hz), 12.44 (s, 1H). ^{13}C NMR (126.0 MHz, DMSO-*d*6) *δ*C: 104.19, 119.18, 123.62, 125.55, 127.63, 128.65, 134.58, 136.75, 141.51, 149.45, 150.69, 153.24, 167.84.

Synthesis of HLS^{2}: HLS^{2} was synthesized in a similar way to **HLS^{1}**, but using 2-bromo-4'-methoxyacetophenone (0.11 g; 0.5 mmol) instead of 2-bromoacetophenone. Yield: 0.12 g (74 %). Anal. Calcd for $C_{16}H_{14}N_4OS$ (%): C,61.92; H, 4.55; N, 18.05; S, 10.33. Found: C, 61.66; H, 4.39; N, 18.22; S, 10.56. IR (ATR, ν_{max}/cm^{-1}): 3186 (w), 3102 (w), 2950 (w), 1567 (s), 1464 (m), 1435 (m), 1353 (m), 1241 (m), 1146 (m), 1030 (w), 912 (w), 832 (m), 732 (m), 696 (m). ^{1}H NMR (500.26 MHz, DMSO-d6) *δ*H: 3.78 (s, 3H), 6.97 (d, 2H, *J* = 8.9 Hz), 7.18 (s, 1H), 7.34 (m, 1H), 7.79 (d, 2H, *J* = 8.9 Hz), 7.83 (m, 1H), 7.86 (m, 1H), 8.06 (s, 1H), 8.57 (d, 1H, *J* = 5.0 Hz), 12.38 (s, 1H). ^{13}C NMR (126.0 MHz, DMSO-*d*6) *δ*C: 55.10, 102.01, 113.98, 119.12, 123.57, 126.85, 127.42, 136.73, 141.36, 149.43, 150.52, 153.24, 158.84, 167.67.

Synthesis of HLS^3: HLS^3 was synthesized, by previously published method,[S5] in a similar way to **HLS^1**, but using 2-bromo-4'-methylacetophenone (0.11 g; 0.5 mmol) instead of 2-bromoacetophenone. Yield: 0.11 g (75 %). Anal. Calcd for $C_{16}H_{14}N_4S$ (%): C, 65.28; H, 4.79; N, 19.09; S, 10.89. Found: C, 65.46; H, 4.84; N, 18.99; S, 10.46. IR (ATR, ν_{max}/cm^{-1}): 3176 (w), 3109 (w), 3066 (w), 2930 (w), 2850 (w), 2717 (m), 1599 (m), 1573 (vs), 1478 (s), 1456 (w), 1431 (w), 1407 (w), 1360 (w), 1298 (w), 1271 (vs, 1148 (s), 1115 (w), 1089 (w), 1047(m), 1000 (m), 913(m), 879 (w), 839 (w), 789 (w), 766 (w), 726 (m), 681 (m), 637 (w). ^{1}H NMR (500.26 MHz, DMSO-d6) δH: 2.31 (s, 3H), 7.21 (d, 2H, J = 8.0 Hz), 7.27 (s, 1H), 7.34 (m, 1H), 7.75 (d, 2H, J = 8.1 Hz), 7.84 (m, 1H), 7.86 (m, 1H), 8.07 (s, 1H), 8.57 (d, 1H, J = 4.5 Hz), 12.40 (s, 1H). ^{13}C NMR (126.0 MHz, DMSO-*d*6) δC: 20.78, 103.22, 119.13, 123.57, 125.46, 129.18, 131.91, 136.71, 136.88, 141.41, 149.43, 150.71, 153.24, 167.70.

Synthesis of 1-Se: Into suspension of **HLSe^1** (0.10 g; 0.30 mmol) in 20 mL of MeOH, solid $Co(BF_4)_2\times6H_2O$ (0.05 g; 0.15 mmol) was added. Obtained rotten cherry solution was refluxed for 1 h. After two days emerald colored single crystals were filtered off, washed with cold MeOH and Et_2O.Yield: 0.07 g (61 %). Anal. Calcd for $C_{30}H_{22}CoN_8Se_2BF_4$ (%):C, 45.14; H, 2.78; N, 14.04. Found: C, 45.42; H, 2.54; N, 13.89. Λ_M (1 × 10^{-3} M, MeOH) = 103.2 Ω^{-1} cm^2 mol^{-1}. IR (ATR, ν_{max}/cm^{-1}): 3054 (w), 1600 (m), 1570 (w), 1540 (m), 1479 (m), 1407 (vs), 1345 (s), 1233 (m), 1126 (s), 1103 (m), 1050 (m), 882 (w), 842 (w), 729 (w). ^{1}H NMR (500.26 MHz, DMSO-d6) δH: 6.75 (s, 1H), 6.75 (d, 2H, J = 6.4 Hz), 7.29 (ddd, 1H, J = 7.4 Hz, J = 5.9 Hz, J = 1.4 Hz), 7.40 (t, 2H, J = 7.8 Hz), 7.49 (d, 1H, J = 5.3 Hz), 7.58 (ddd, 1H, J = 7.5 Hz, J = 6.4 Hz, J = 1.2 Hz), 7.68 (dd, 1H, J = 8.0 Hz, J = 0.8 Hz), 7.82 (s, 1H), 7.95 (td, 1H, J = 7.7, Hz, J = 1.3 Hz). ^{13}C NMR (126.0 MHz, DMSO-*d*6) δC: 110.90, 123.68, 125.99, 127.66, 128.89, 129.30, 133.13, 139.52, 141.26, 148.22, 149.33, 159.94, 183.60.

Synthesis of 2-Se: 2-Se was synthesized in a similar way to **1-Se**, but using **HLSe^2** (0.11 g; 0.30 mmol) instead of **HLSe^1**. XRD quality single crystals were obtained by diffusion of EtOAc vapor into the solution of **2-Se** in DMSO. Yield: 0.07 g (57 %). Anal. Calcd for $C_{32}H_{26}CoN_8O_2Se_2BF_4H_2O$ (%): C, 43.86; H, 3.22; N, 12.79. Found: C, 43.52; H, 2.93; N, 12.87;. Λ_M (1 × 10^{-3} M, MeOH) = 82.4 Ω^{-1} cm^2 mol^{-1}. IR (ATR, ν_{max}/cm^{-1}): 3114 (w), 2962 (w), 2836 (w), 1603 (m), 1526 (m), 1477 (m), 1390 (s), 1340 (s), 1238 (s), 1128 (s), 1053 (s), 886 (m), 831 (m), 742 (w), 671 (w), 515 (w). ^{1}H NMR (500.26 MHz, DMSO-d6) δH: 3.89 (s, 3H), 6.65 (d,

2H, *J* = 8.4 Hz), 6.69 (s, 1H), 6.93 (d, 2H, *J* = 8.6 Hz), 7.29 (ddd, 1H, *J* = 7.2 Hz, *J* = 6.1 Hz, *J* = 0.9 Hz), 7.50 (d, 1H, *J* = 5.7 Hz), 7.69 (d, 1H, *J* = 7.7 Hz), 7.90 (s, 1H), 7.95 (td, 1H, *J* = 7.9 Hz, *J* = 0.8 Hz). ^{13}C NMR (126.0 MHz, DMSO-*d*6) *δ*C: 55.28, 110.57, 112.90, 123.49, 125.29, 125.77, 130.08, 139.11, 141.09, 147.97, 149.17, 159.94, 183.19.

Synthesis of 3-Se: 3-Se was synthesized in a similar way to **1-Se**, but using **HLSe[3]** (0.10 g; 0.30 mmol) instead of **HLSe[1]**. Yield: 0.07 g (58 %). Anal. Calcd for $C_{32}H_{26}CoN_8Se_2BF_4$ (%): C, 46.52; H, 3.17; N, 13.56. Found: C, 46.74; H, 2.98; N, 13.82. Λ_M (1 × 10^{-3} M, MeOH) = 110.6 Ω^{-1} cm^2 mol^{-1}. IR (ATR, ν_{max}/cm^{-1}): 3128 (w), 3082 (w), 1602 (m), 1530 (m), 1481 (m), 1393 (s), 1342 (s), 1318 (m), 1239 (m), 1131 (m), 1055 (s), 885 (w), 847 (w), 740 (w), 669 (w), 517 (w). ^{1}H NMR (500.26 MHz, DMSO-d6) *δ*H: 2.46 (s, 3H), 6.62 (d, 2H, *J* = 7.7 Hz), 6.68 (s, 1H), 7.19 (d, 2H, *J* = 7.6 Hz), 7.28 (ddd, 1H, *J* = 7.4 Hz, *J* = 5.9 Hz, *J* = 1.4 Hz), 7.48 (d, 1H, *J* = 5.5 Hz), 7.68 (dd, 1H, *J* = 7.9 Hz, *J* = 0.6 Hz), 7.83 (s, 1H), 7.94 (td, 1H, *J* = 7.8 Hz, *J* = 1.3 Hz). ^{13}C NMR (126.0 MHz, DMSO-d6) *δ*C: 21.05, 110.54, 123.42, 125.71, 127.92, 128.59, 130.16, 138.36, 139.19, 141.05, 148.12, 149.07, 159.85, 183.31.

Synthesis of 1-S: 1-S was synthesized in a similar way to **1-Se**, but using **HLS[1]** (0.08 g; 0.30 mmol) instead of **HLSe[1]**. Yield: 0.11 g (65 %). Anal. Calcd for $C_{30}H_{22}CoN_8S_2BF_4$ (%): C, 51.15; H, 3.15; N, 15.91; S, 9.10. Found: C, 51.07; H, 3.24; N,15.72; S, 9.35. Λ_M (1 × 10^{-3} M, MeOH) = 94.4 Ω^{-1} cm^2 mol^{-1}. IR (ATR, ν_{max}/cm^{-1}): 3055 (w), 1600 (m), 1570 (w), 1539 (m), 1478 (m), 1396 (s), 1346 (s), 1237 (s), 1129 (s), 1044 (s), 901 (w), 753 (w), 696 (w), 661 (w). ^{1}H NMR (500.26 MHz, DMSO-d6) *δ*H: 6.56 (s, 1H), 6.77 (d, 2H, *J* = 6.9 Hz,), 7.29 (ddd, 1H, *J* = 7.3 Hz, *J* = 6.1 Hz, *J* = 1.3 Hz), 7.42 (t, 2H, *J* = 7.7 Hz), 7.53 (d, 1H, *J* = 5.6 Hz), 7.60 (t, 1H, *J* = 7.5 Hz), 7.66 (d, 1H, *J* = 7.4 Hz), 7.82 (s, 1H), 7.96 (td, 1H, *J* = 7.8, Hz, *J* = 1.2 Hz). ^{13}C NMR (126.0 MHz, DMSO-*d*6) *δ*C: 108.12, 123.28, 126.06, 127.73, 128.78, 129.54, 131.63, 139.47, 141.27, 147.89, 149.19, 159.81, 180.47.

Synthesis of 2-S: 2-S was synthesized in a similar way to **1-Se**, but using **HLS[2]** (0.09 g; 0.30 mmol) instead of **HSe[1]**. Yield: 0.07 g (63 %). Anal. Calcd for $C_{32}H_{26}CoN_8O_2S_2BF_4$ (%): C, 50.28; H, 3.43; N, 14.66; S, 8.39. Found: C, 50.55; H, 3.32; N, 14.78; S, 8.07. Λ_M (1 × 10^{-3} M, MeOH) = 102.2 Ω^{-1} cm^2 mol^{-1}. IR (ATR, ν_{max}/cm^{-1}): 3148 (w), 3079 (w), 3042 (w), 1602 (m), 1531 (m), 1494 (m), 1394 (s), 1344 (m), 1323 (m), 1243 (s), 1133 (m), 1105 (m), 1049 (m), 1019 (m), 904 (w), 820 (w), 778 (w). ^{1}H NMR (500.26 MHz, DMSO-d6) *δ*H: 3.23 (s, 3H), 6.47 (s,

1H), 6.65 (d, 2H, J = 8.6 Hz), 6.94 (d, 2H, J = 8.6 Hz), 7.27 (ddd, 1H, J = 7.3 Hz, J = 6.1 Hz, J = 1.3 Hz), 7.53 (d, 1H, J = 5.6 Hz), 7.65 (d, 1H, J = 7.9 Hz), 7.87 (s, 1H), 7.94 (td, 1H, J = 7.8 Hz, J = 1.2 Hz). ^{13}C NMR (126.0 MHz, DMSO-*d*6) δC: 55.55, 108.06, 113.29, 123.39, 124.01, 126.08, 130.30, 139.33, 141.39, 147.98, 149.29, 160.06, 160.42, 180.45.

Synthesis of 3-S: 3-S was synthesized, according to the literature procedure,[S5] in a similar way to **1-Se**, but using **HLS^3** (0.09 g; 0.30 mmol) instead of **HLSe^1**. Yield: 0.07 g (67 %). Anal. Calcd for (%): C, 52.47; H, 3.58; N, 15.30; S, 8.76. Found: C, 52.46; H, 3.39; N, 15.40; S, 8.84. Λ_M (1 × 10^{-3} M, MeOH) = 89.10 Ω^{-1} cm^2 mol^{-1}. IR (ATR, ν_{max}/cm^{-1}): 3548 (w), 3128 (w), 3074 (w), 1603 (m), 1570 (w), 1533 (s), 1486 (m), 1444 (w), 1400 (vs), 1346 (vs), 1326 (w),1245 (s), 1136 (w), 1055 (m), 935 (w), 906 (m), 846 (w), 811 (m), 766 (m), 676 (w), 637 (w). ^{1}H NMR (500.26 MHz, DMSO-*d*6) δH: 2.46 (s, 3H), 6.50 (s, 1H), 6.64 (d, 2H, ^3J = 8.0 Hz), 7.21 (d, 2H, ^3J = 8.0 Hz), 7.28 (ddd, 1H, ^3J = 7.4 Hz, ^3J = 5.7 Hz, ^3J = 1.4 Hz), 7.52 (d, 1H, ^3J = 5.4 Hz), 7.65 (dd, 1H, ^3J = 8.0 Hz, ^3J = 0.8 Hz), 7.82 (s, 1H), 7.99 (td, 1H, J = 7.8 Hz, ^3J = 1.3 Hz). ^{13}C NMR (126.0 MHz, DMSO-d6) δC: 21.19, 107.98, 123.22, 125.98, 128.22, 128.66, 128.84, 138.90, 139.35, 141.01, 148.01, 149.12, 159.91, 180.43.

X-ray crystallography

The single-crystal X-ray diffraction data were collected on a Gemini S diffractometer (Oxford Diffraction) equipped with a Sapphire CCD detector. Graphite monochromated Mo *Kα* radiation was employed in all experiments. The *CrysAlisPro*[S6] was used for raw data integration and reduction. Structures were solved by using *SHELXT*,[S7]and refined by *SHELXL-2015*[S8] program. The *SHELXLE*[S9] was used as a graphical user interface for refinement procedures. All non-hydrogen atoms were refined anisotropically, while hydrogen atoms were treated by a riding model in geometrically idealized positions, with their $U_{iso} = kU_{eq}$ of their parent atoms(k = 1.5 for CH_3, 1.2 for all other hydrogen atoms). In complex **2-Se**, hydrogen atoms belonging to water molecule could not be located in the electron density maps.

In complex **3-Se**, the BF_4^- ion is modeled as disordered between two positions. Common occupational numbers were refined for oxygen atoms belonging to two orientations. Distance and ADP similarity restraints were employed in the refinement to achieve reasonable geometry.

Diffraction pattern of **3-S** specimen showed 6/*mmm* symmetry, however, the structure could not be solved in hexagonal space groups. Closer inspection of the diffraction data revealed several signs of twinning.[S10] The structure was solved in trigonal $P3_121$ space group using *SIR*92,[S11] but it could not be adequately refined. The analysis with *TWINROTMAT* in *PLATON* [S12] indicated twinning by merohedry with thetwin law −1 0 0, 0 −1 0, 0 0 1. The structure was therefore refined as a four-component twin as described in literature.[S13,S14]

A summary of the crystallographic data is given in Table S1. Structures were validated with the *PLATON*, [S12] and extensive use of the Cambridge Structural Database System.[S15] Crystallographic data for the complexes have been deposited with the Cambridge Crystallographic Data Centre as Supplementary Publication No. CCDC 1523111-1523115. A copy of these data can be obtained, free of charge, via https://summary.ccdc.cam.ac.uk/structure-summary-form, or by emailing data_request@ccdc.cam.ac.uk.

Cyclic voltammetry and spectroelectrochemistry

The cyclic voltammetry experiments were done on a PST050 Voltalab instrument. Three-electrode cell consisted of a glassy carbon (GC) disk electrode (3 mm) polished with alumina suspension before each voltammetric curve, Pt wire counter electrode and a saturated calomel electrode (SCE) as a reference one. Voltammetric measurements were done in a potential range + 1.5 V to – 2.1 V, applying sweep rates from 0.010 V/s to 2 V/s. The solutions of the compounds (0.2 $mmoldm^{-3}$ – 1.2 $mmoldm^{-3}$) were prepared in doubly distilled *N*,*N*-dimethylformamide (DMF) with tetrabutylammonium perchlorate (TBAP) as supporting electrolyte. The solutions were carefully deaerated by purging nitrogen before an experiment and a strong stream of the gas was maintained during the measurements.

Spectroelectrochemical spectra were recorded on a Cary 100scan UV-visible spectrophotometer with a μ-Autolab type III potentiostat. Herein, spectroelectrochemical cell was constructed by loading a transparent Pt grid working electrode into 1mm path length thin layer channel in the quartz cuvette and mounting the other two electrodes above the channel.

Computational methodology

All the quantum chemical calculations for investigated ligands and complexes were performed under the density functional theory (DFT), using the Gaussian 09 program package.[S16] Initial geometries of neutral *E*- and *Z*-isomeric form of ligands were optimized with Becke's gradient-corrected exchange correlation in conjunction with the Lee-Yang-Parr correlation functional with three parameters (B3LYP), [S17,S18] while the full geometry optimizations of the crystal structures of Co(III) complexes were carried out using BP86 (the Gaussian program specified as BVP86) [S19– S21] functional, in the gas phase. Polarized 6-31G(d,p) basis set for Co atom and 6-31G(d) for N, C, O, S, Se and H atoms were used in all theoretical calculations. [S22–S25] The stability of optimized geometries was confirmed by the frequency calculations, which were obtained without any imaginary wavenumber values, at the selected level of theory for ligands and complexes. The gas phase calculated molecular structures were re-optimized in DMF and DMSO solvent using the polarisable continuum model (PCM)[S26] with the B3LYP and BVP86 functionals for ligands and complexes, respectively. Theoretical NMR chemical shifts were calculated at DFT/B3LYP level of theory using Gauge-Independent Atomic Orbital (GIAO)[S27] approximation in DMSO, as a solvent. The absorption spectra and the transition energy evaluations were carried out within time dependent density functional theory (TD-DFT) approach, using B3LYP functional and DMF solvent. Since the parameters for the DMF solvent are not specified in SCRF module in Gaussian program, following the previous studies, [S28,S29] the DMF was specified with the parameters: ε = 36.71, numeral density = 0.00778 particles $Å^{-3}$, epsinf = 1.75, rsolv = 2.647 Å and vmol = 77.4 cm^3 mol^{-1}.

In addition, the Fukui function was used to illustrate the electrophilicity of the several atoms of investigated ligands and compexes. Parr and Yang showed that sites in chemical species with the largest values of Fukui Function f(r) are those with higher reactivity. The Fukui $f(r)$ function is defined as: [S30,S31]

$$f(r)=\left(\frac{\partial\rho(r)}{\partial N}\right)_{v}$$

where $\rho(r)$ is the total electron density of the molecule, N is the number of electrons and r is the

external potential exerted by the nucleus. Thus, the condensed Fukui function of the atom A in a molecule with N electrons can be defined as:

$$f_A^+ = q_N^A - q_{N+1}^A \quad \text{for nucleophilic attack} \quad (1)$$

$$f_A^- = q_{N-1}^A - q_N^A \quad \text{for electrophilic attack} \quad (2)$$

where, q_N^A , q_{N+1}^A and q_{N-1}^A are the electronic population of the atom A in neutral, anionic and cationic forms, respectively.

The above the electronic population can be obtained from the natural bond orbital (NBO) calculations. [S32]

Antimicrobial activity

The antimicrobial activity was determinated using four different strains of the Gram-positive bacteria: *Staphylococcus aureus* (ATCC 6538), *Kocuria rhizophila* (ATCC 9341), *Clostridium sporogenes* (ATCC 19404), *Bacillus subtilis* (ATCC 6633), four different strains of the Gram-negative bacteria: *Escherichia coli* (ATCC 25922), *Salmonella enterica* subsp. *enterica* serovar Enteritidis (ATCC 13076), *Proteus hauseri* (ATCC 13315), *Pseudomonas aeruginosa* (ATCC 9027) and three strains of the fungi: *Candida albicans* (ATCC 10231), *Sacharomyces cerevisiae* (ATCC 9763) and *Aspergillus brasiliensis* (ATCC 16404). Antimicrobial activity was determinated by well diffusion method.[S33] In each Petri dish (90mm diameter) 22 mL of Nutrient agar (Hi Media, Mumbai, India) and 100 µL of bacterial suspension (10^6 cells/dish) were added, while for antifungal activity in each sterile Petri dish (90 mm diameter) 22 mL of Sabouraud dextrose agar suspension (Torlak, Belgrade, Serbia) was poured and 100 µL of fungi (10^5 spores/dish) were added. Eight milimeter diameter well was then punched carefully using a sterile cork borer and 100 µL of test substance (1 mg/100 µL DMSO) were added into each labeled well. Amikacin (30 µg/100 µL H_2O) was used as a positive control for bacteria, nystatin (30 µg/100 µL DMSO) was used as a positive control for fungi, while 100 µL of water and DMSO served as a negative controls. The same procedure was repeated for

different microorganisms. After the inoculation of the organisms, compounds and controls, the plates were incubated for 24 h at 37 °C for bacteria and 48 h at 28 °C for fungi. Antimicrobial activity was determinated by measuring the diameter of inhibition zone. Zones of inhibition were recorded in mm.

***Artemia salina* cytotoxicity test**

A teaspoon of lyophilized eggs of the brine shrimp *Artemia salina* was added to 1 L of the artificial sea water containing several drops of yeast suspension (3 mg of dry yeast in 5 mL distilled water), and air was passed through the suspension thermostated at 301 K, under illumination for 24 h. The tested substances were dissolved in DMSO. In a glass vial, into 1 mL of artificial sea water 1–2 drops of yeast extract solution (3 mg in 5 mL of distilled water) and 10–20 hatched nauplii were added, and finally solutions of all derivatives to the appropriate concentrations. For each concentration, three determination were performed. The vials were left at 301 K under illumination for 24 h, and afterwards live and dead nauplii were counted. LC_{50} was defined as the concentration of a drug that causes death of 50 % nauplii. DMSO was inactive under applied conditions.

Free-radical scavenging antioxidant assay (DPPH method)

The proton donating ability was assayed using a protocol for the determination of radical scavenging activity. Compounds were dissolved in pure DMSO and were diluted into ten different concentrations. Commercially available free radical DPPH was dissolved in methanol at a concentration of 6.58×10^{-5} M. Into a 96-well microplate, 140 μL of DPPH solution was loaded and 10 μL DMSO solution of the tested compounds was added, or pure DMSO (10 μL) as the control. The microplate was incubated for 30 min at 298 K in the dark and the absorbance was measured at 517 nm. All the measurements were carried out in triplicate. The scavenging activity of the compounds was calculated using the eq. (1):

$$\text{Scavenging activity (\%)} = (A_{control} - A_{sample})/A_{control} \times 100 \qquad (4)$$

where A_{sample} and $A_{control}$ refer to the absorbances at 517 nm of DPPH in the sample and control solutions, respectively. IC_{50} values were calculated from the plotted graph of scavenging activity against the concentrations of the samples. IC_{50} is defined as the total antioxidant concentration

necessary to decrease the amount of the initial DPPH radical by 50 %. IC_{50} was calculated for all compounds based on the percentage of DPPH radicals scavenged. Ascorbic acid was used as the reference compound (positive control) with concentrations 50 to 500 mg mL^{-1}.

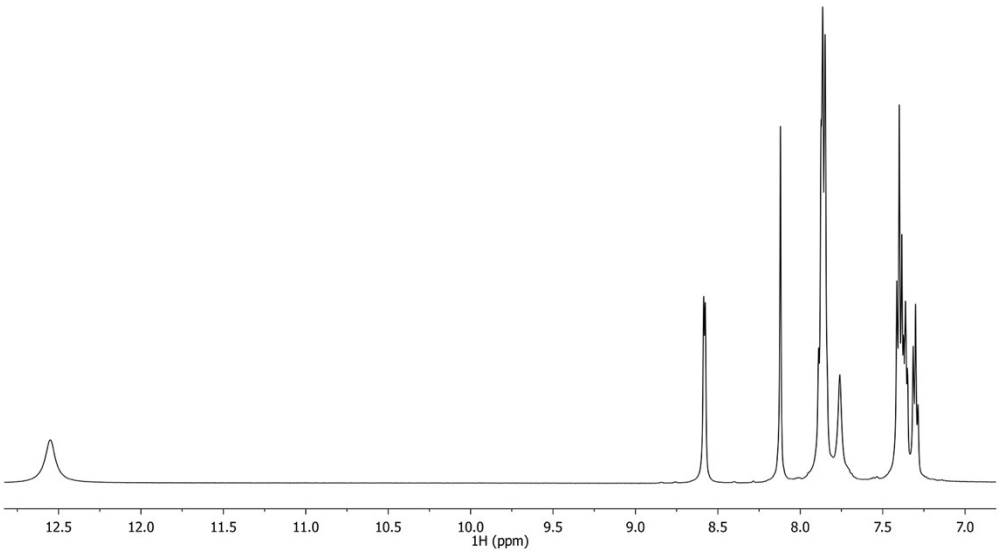

Fig. S1 ^{1}H NMR spectrum of **HLSe[1]** in DMSO-d_6

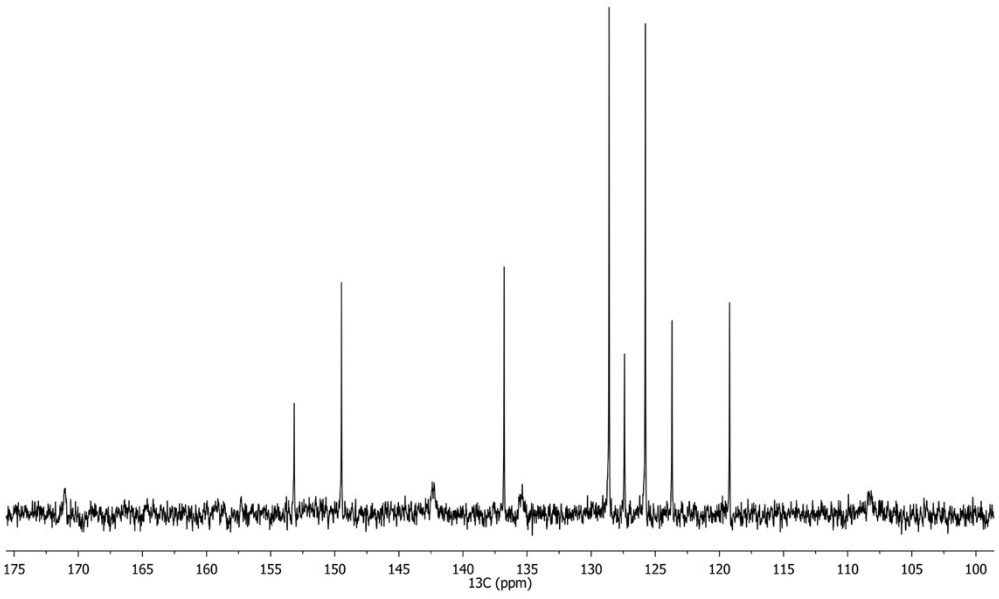

Fig. S2 ^{13}C NMR spectrum of **HLSe[1]** in DMSO-d_6

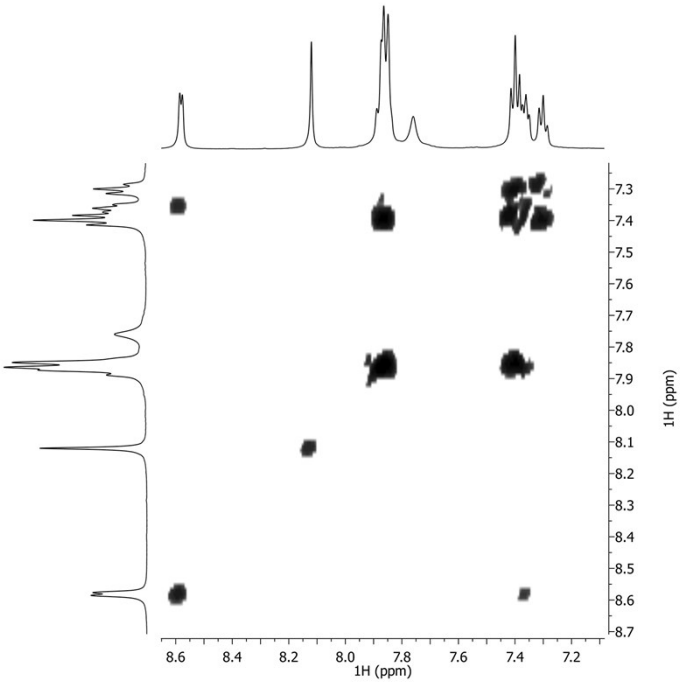

Fig. S3 2D COSY spectrum of **HLSe[1]** in DMSO-d_6

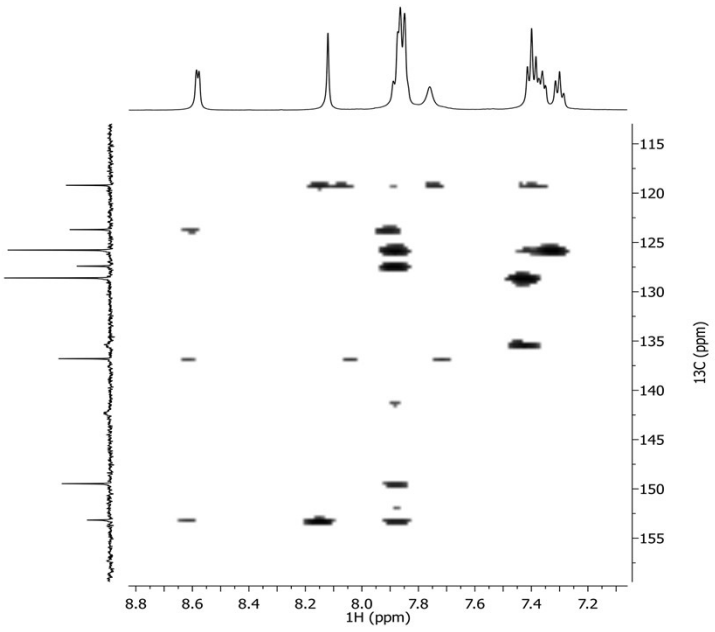

Fig. S4 2D HMBC spectrum of **HLSe[1]** in DMSO-d_6

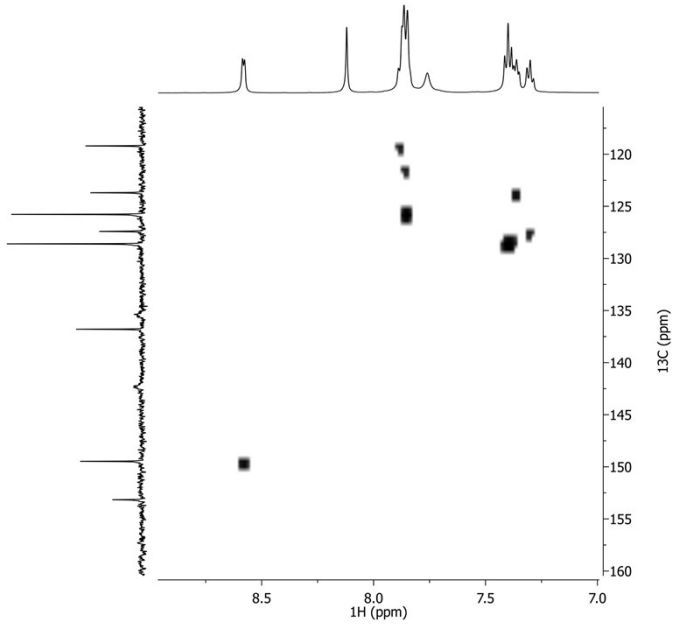

Fig. S5 2D HSQC spectrum of **HLSe[1]** in DMSO-d_6

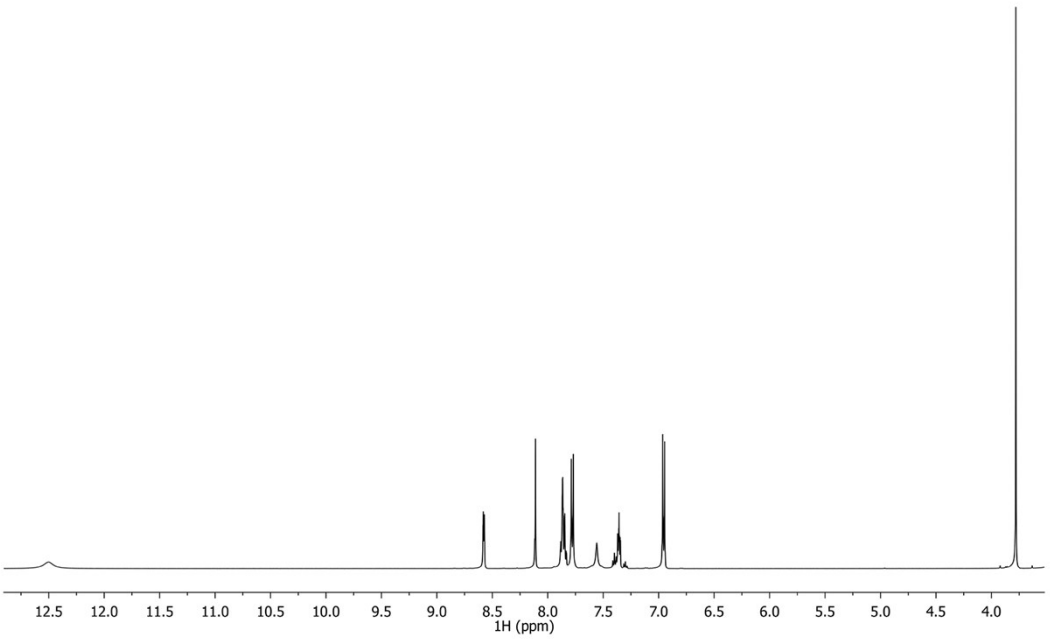

Fig. S6 ^{1}H NMR spectrum of **HLSe[2]** in DMSO-d_6

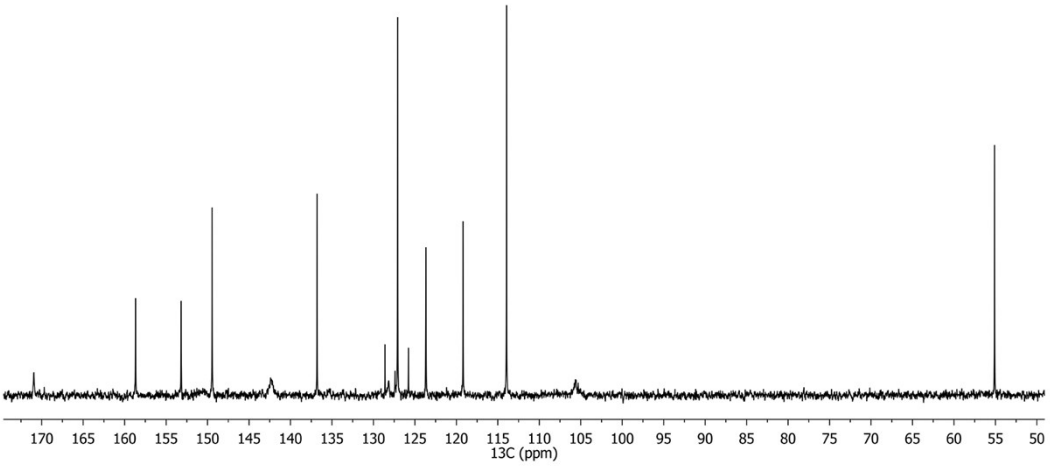

Fig. S7 ^{13}C NMR spectrum of **HLSe²** in DMSO-d_6

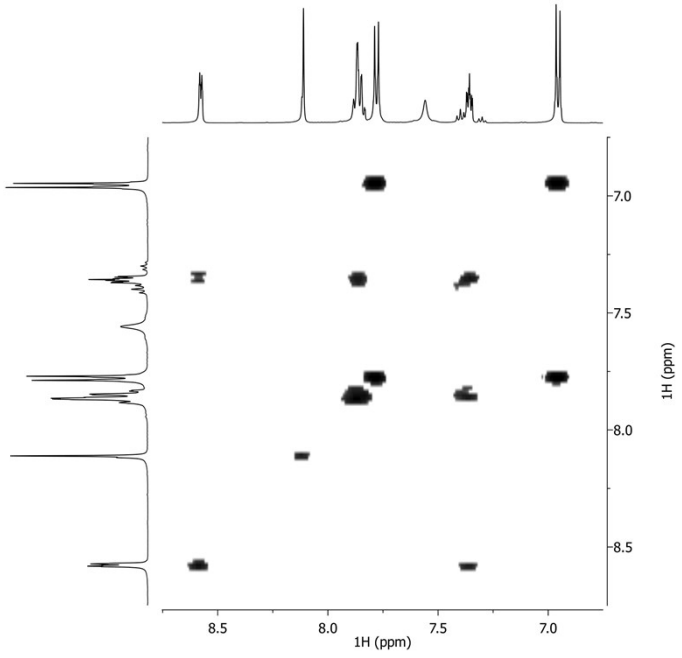

Fig. S8 2D COSY spectrum of **HLSe²** in DMSO-d_6

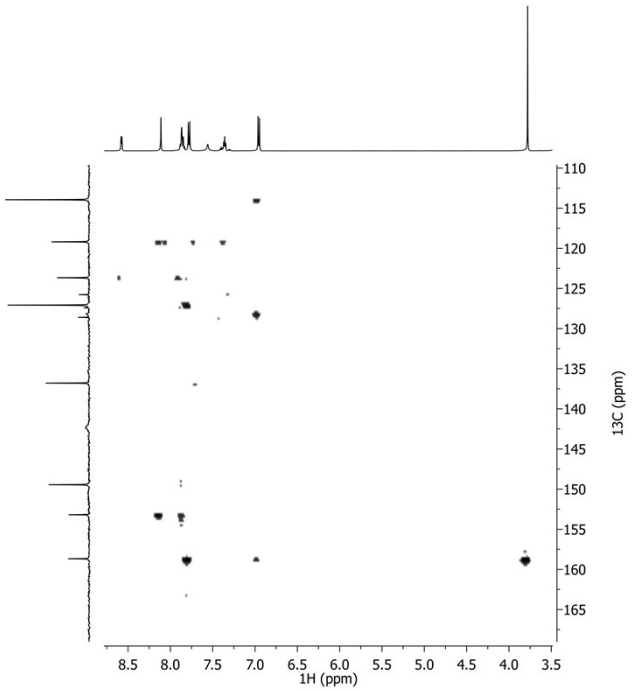

Fig. S9 2D HMBC spectrum of **HLSe²** in DMSO-d_6

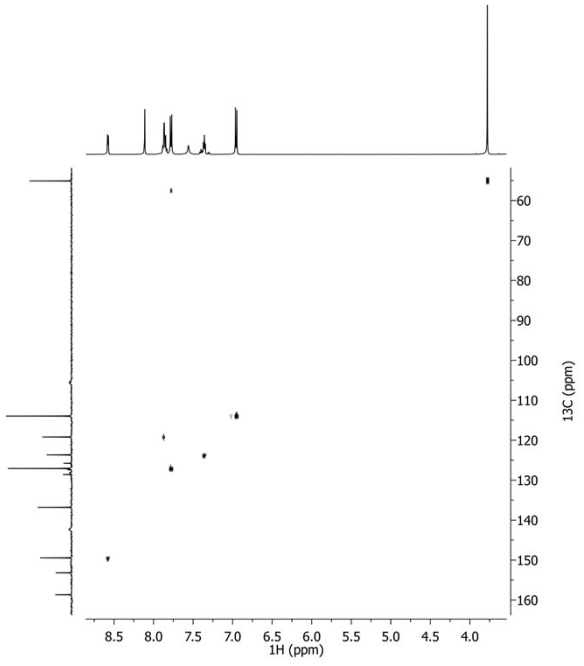

Fig. S10 2D HSQC spectrum of **HLSe²** in DMSO-d_6

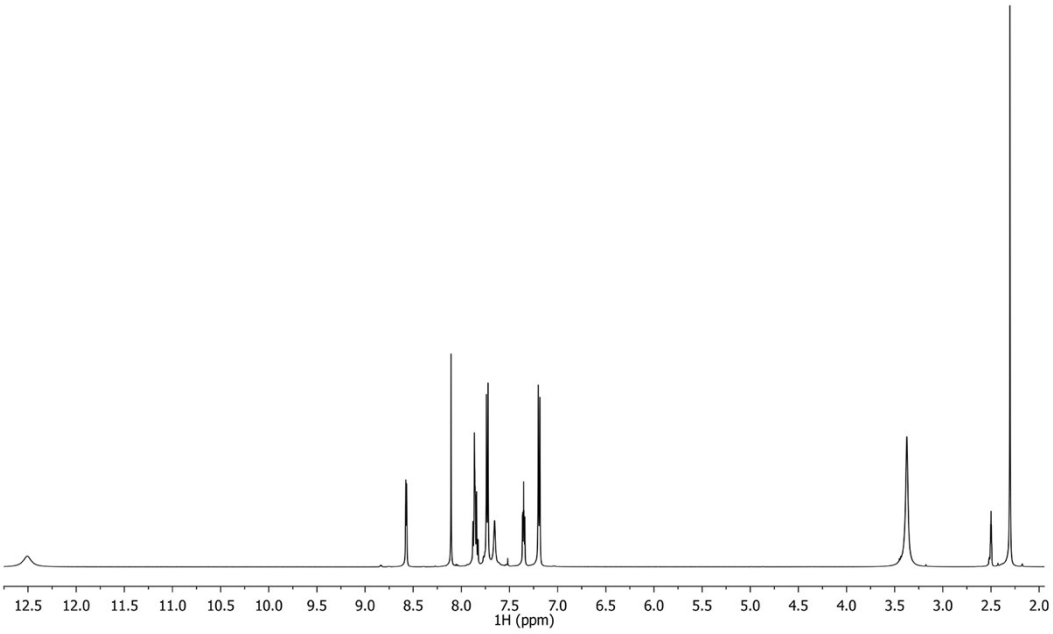

Fig. S11 ^{1}H NMR spectrum of **HLSe^{3}** in DMSO-d_6

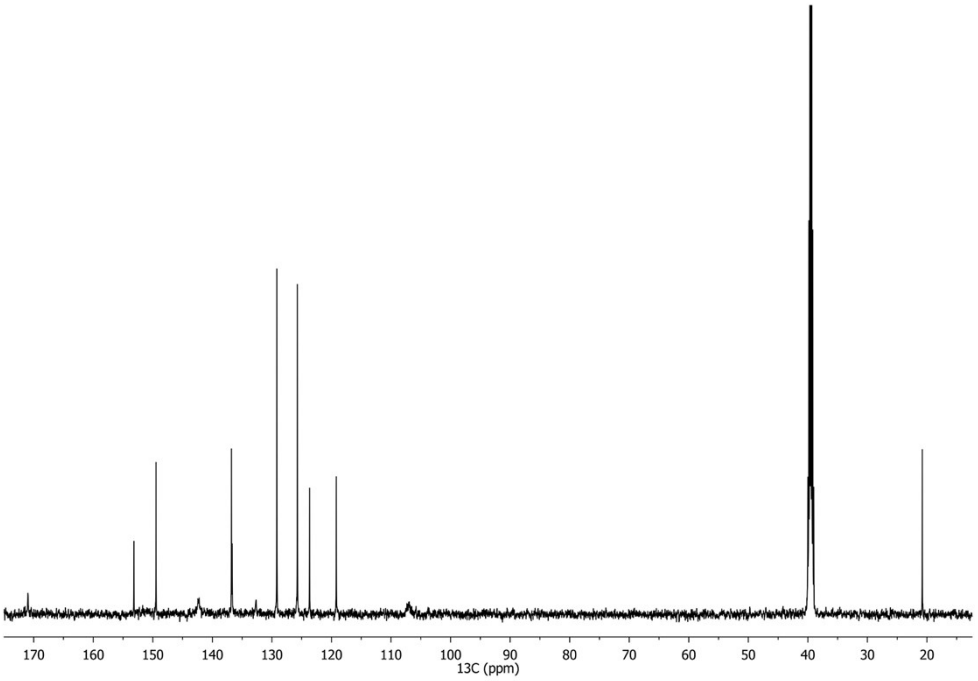

Fig. S12 ^{13}C NMR spectrum of **HLSe^{3}** in DMSO-d_6

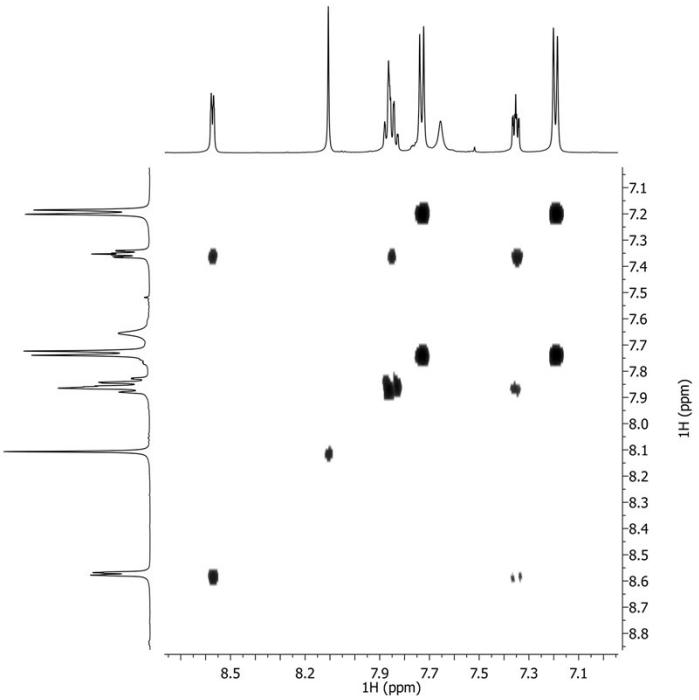

Fig. S13 2D COSY spectrum of **HLSe^3** in DMSO-d_6

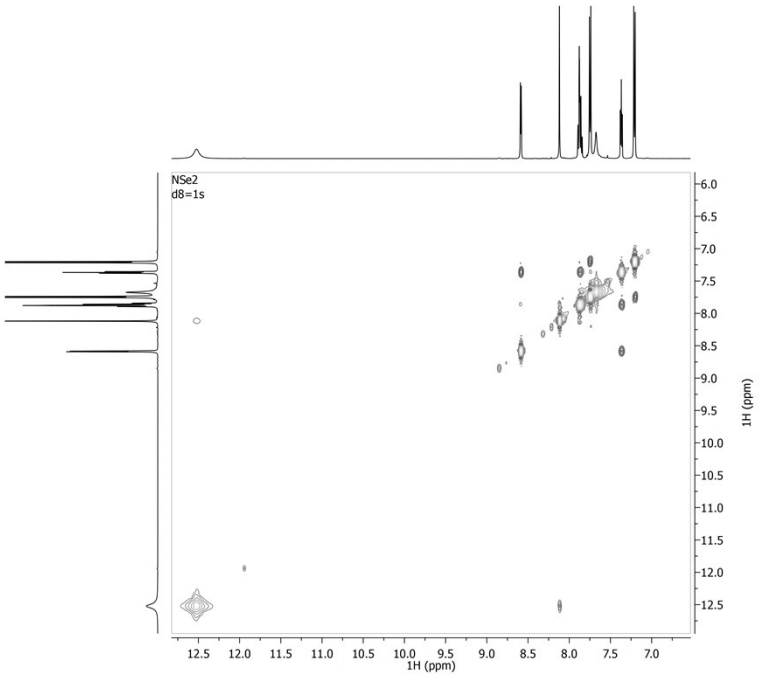

Fig. S14 2D NOESY spectrum of **HLSe^3** in DMSO-d_6

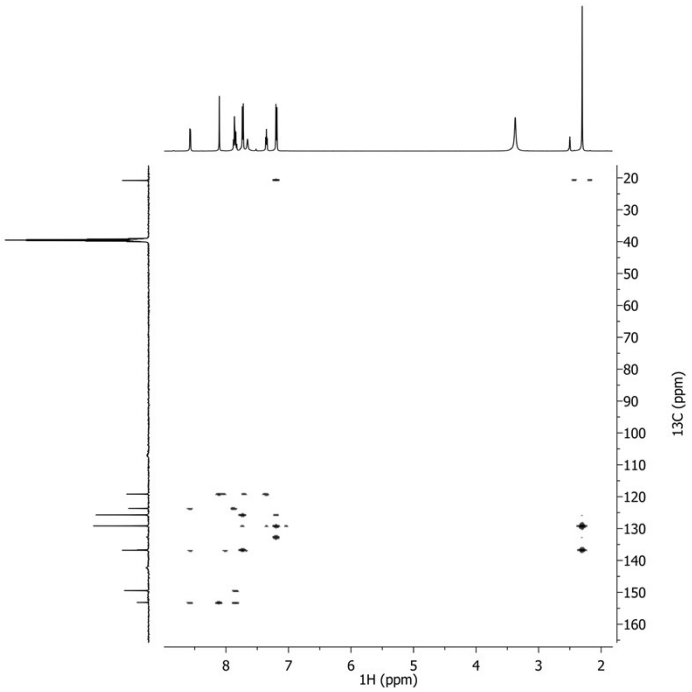

Fig. S15 2D HMBC spectrum of **HLSe[3]** in DMSO-d_6

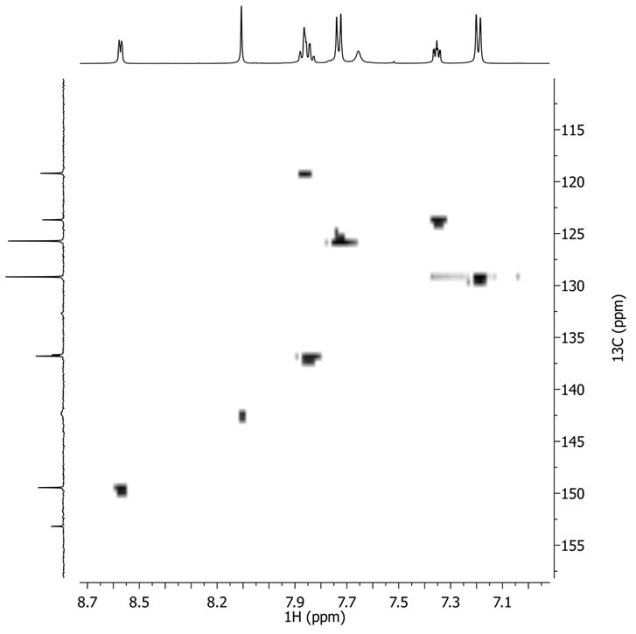

Fig. S16 2D HSQC spectrum of **HLSe[3]** in DMSO-d_6

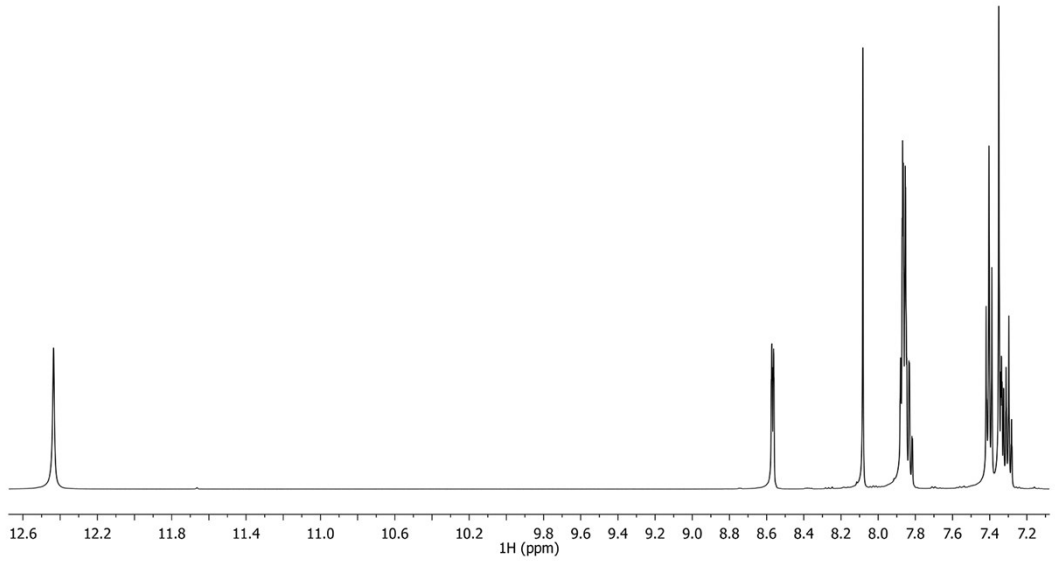

Fig. S17 ^{1}H NMR spectrum of **HLS[1]** in DMSO-d_6

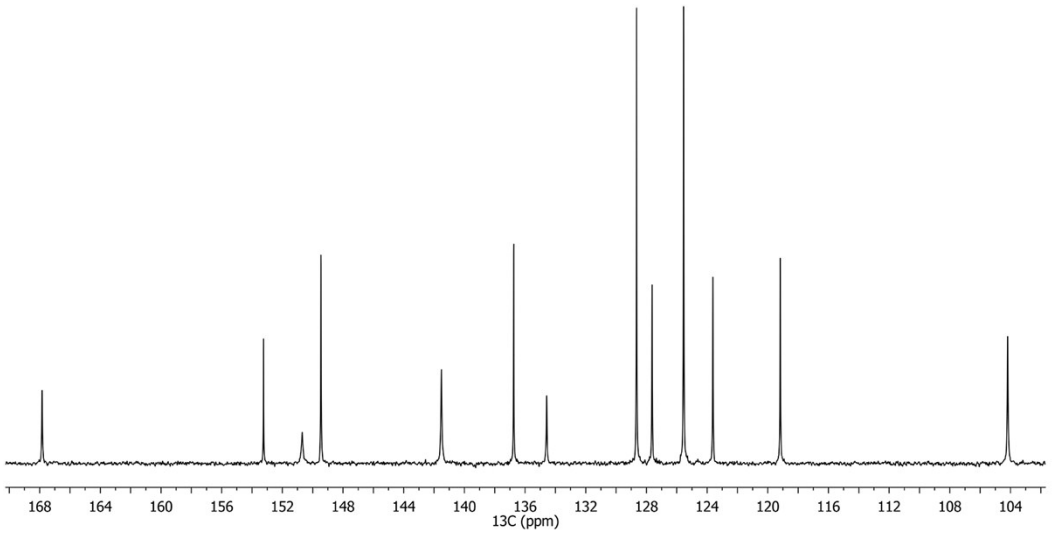

Fig. S18 ^{13}C NMR spectrum of **HLS[1]** in DMSO-d_6

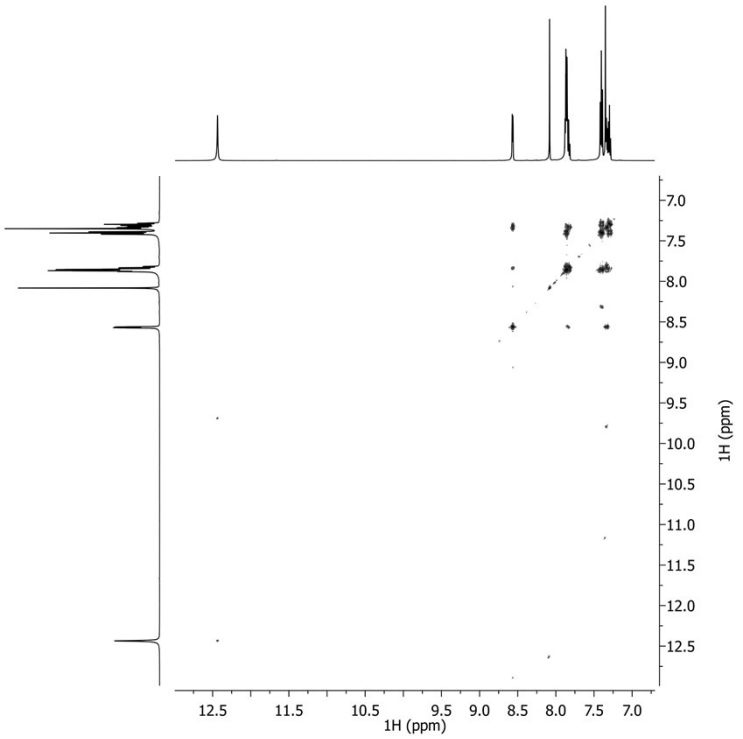

Fig. S19 2D COSY spectrum of **HLS[1]** in DMSO-d_6

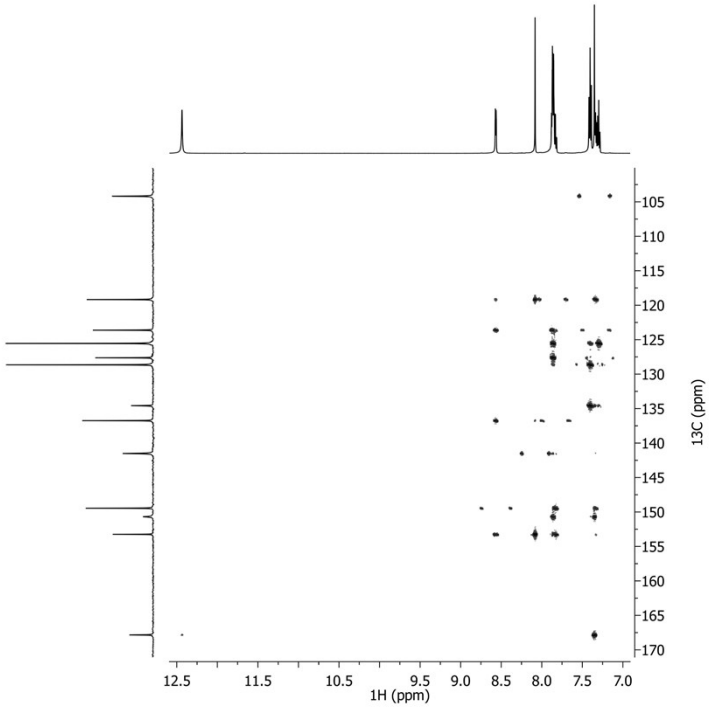

Fig. S20 2D HMBC spectrum of **HLS[1]** in DMSO-d_6

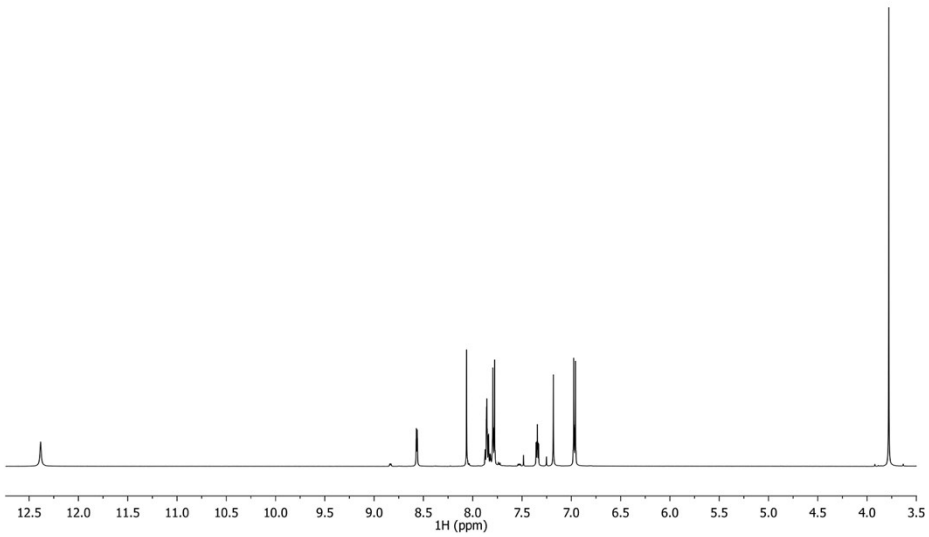

Fig. S21 ^{1}H NMR spectrum of **HLS^{2}** in DMSO-d_6

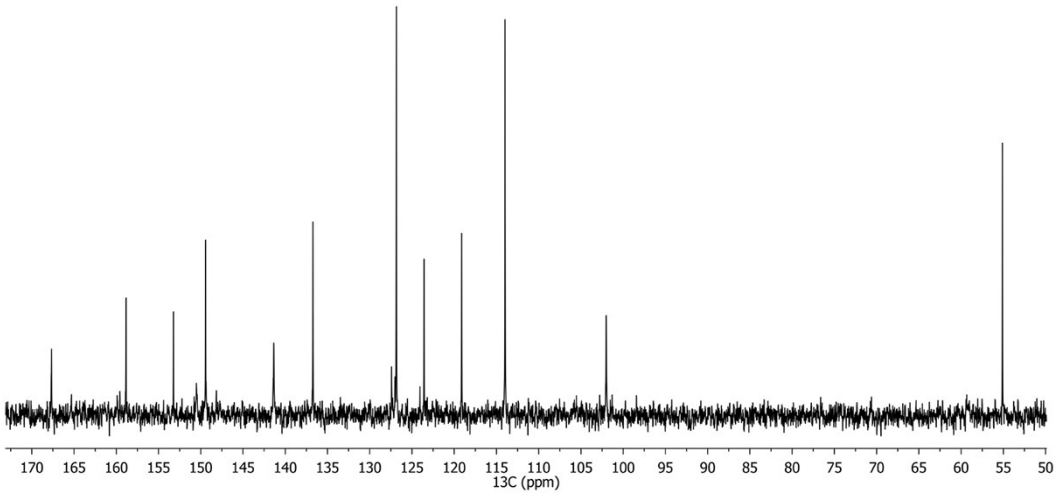

Fig. S22 ^{13}C NMR spectrum of **HLS^{2}** in DMSO-d_6

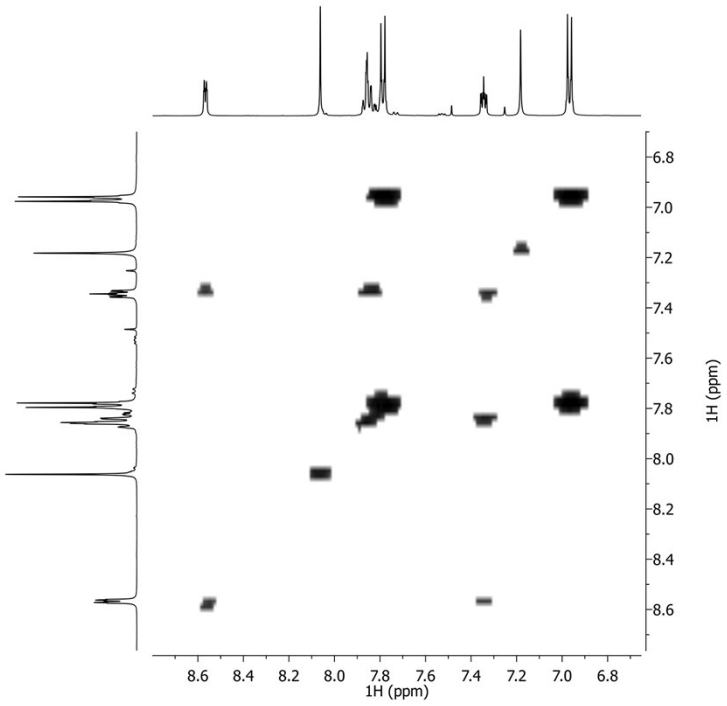

Fig. S23 2D COSY spectrum of **HLS²** in DMSO-d_6

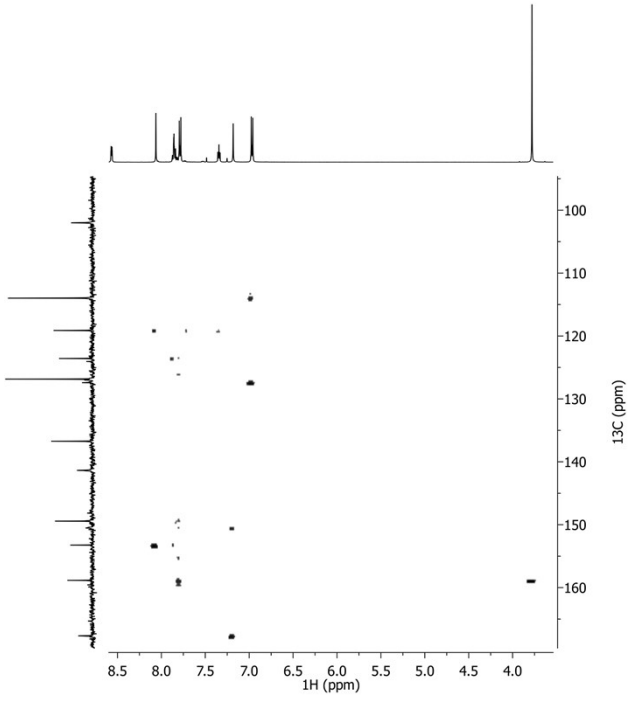

Fig. S24 2D HMBC spectrum of **HLS²** in DMSO-d_6

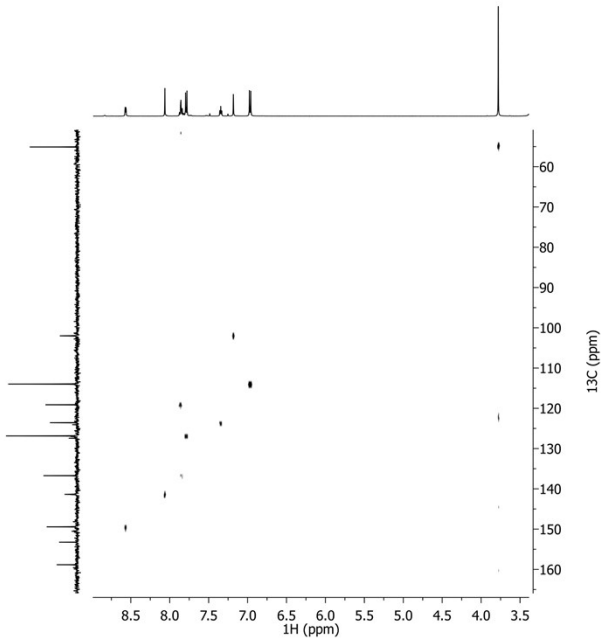

Fig. S25 2D HSQC spectrum of **HLS²** in DMSO-d_6

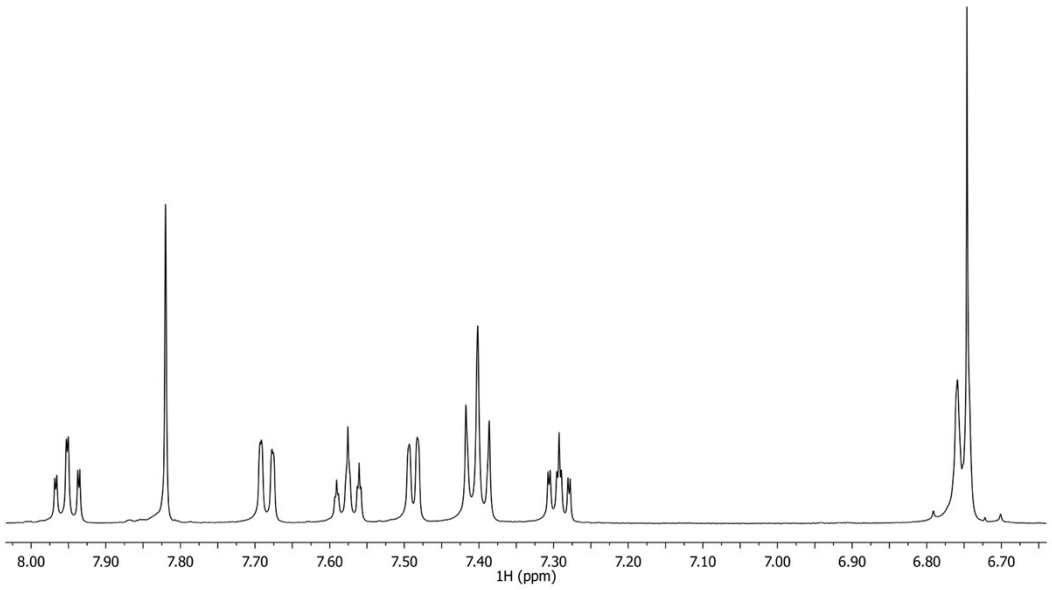

Fig. S26 ^{1}H NMR spectrum of **1-Se** in DMSO-d_6

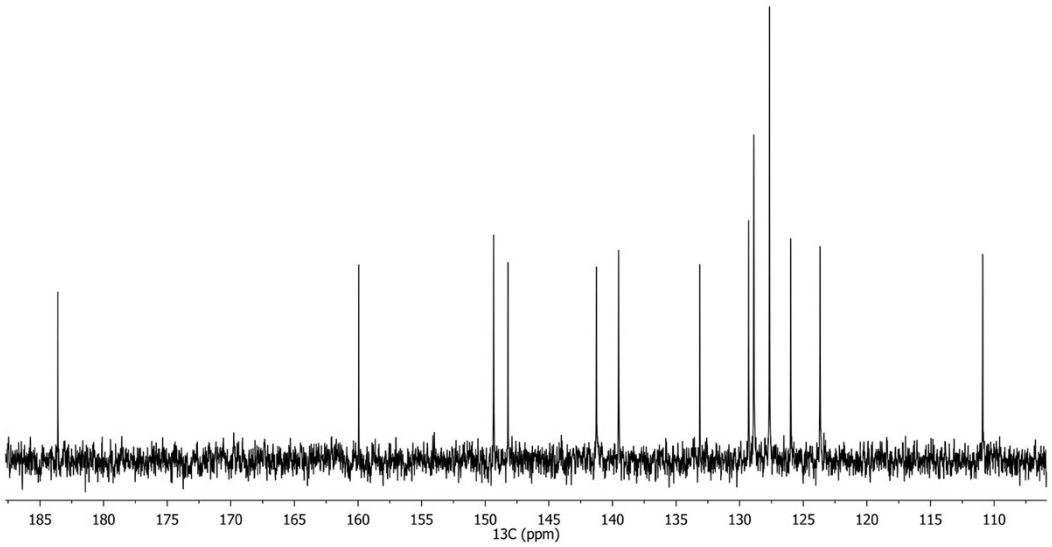

Fig. S27 ^{13}C NMR spectrum of **1-Se** in DMSO-d_6

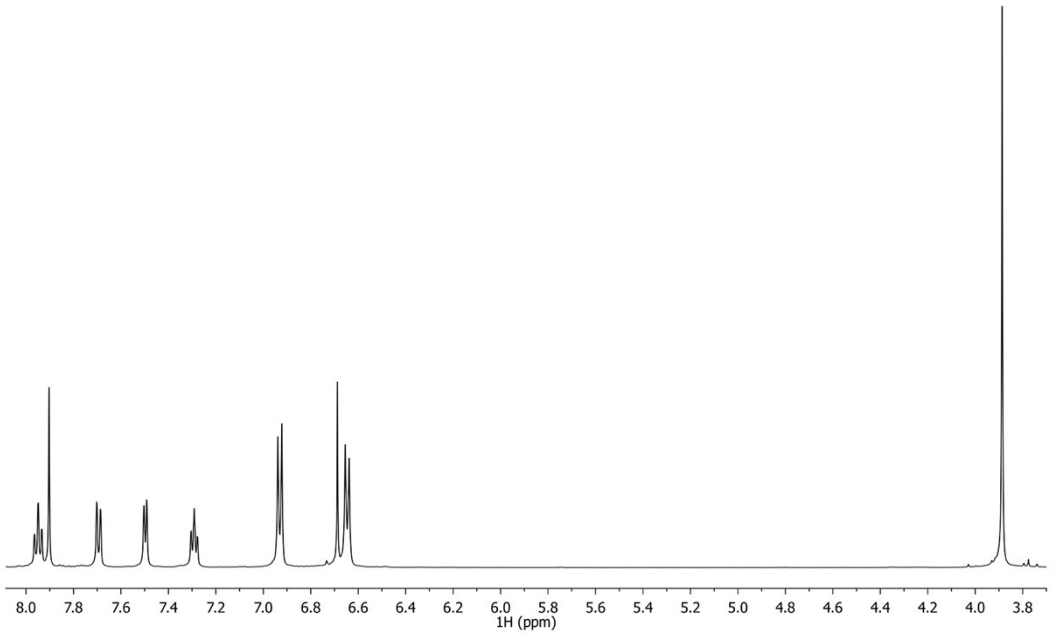

Fig. S28 ^{1}H NMR spectrum of **2-Se** in DMSO-d_6

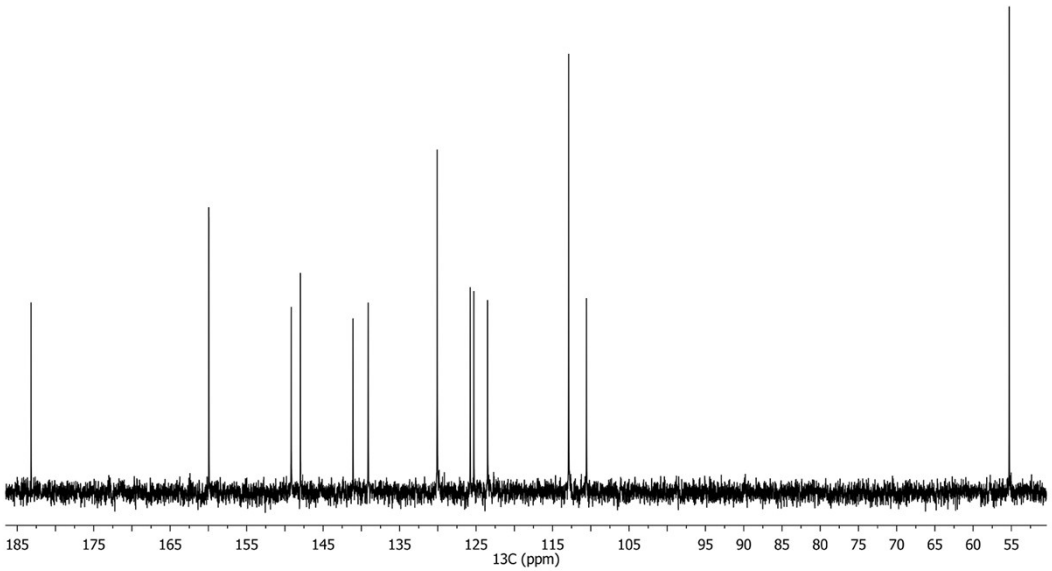

Fig. S29 ^{13}C NMR spectrum of **2-Se** in DMSO-d_6

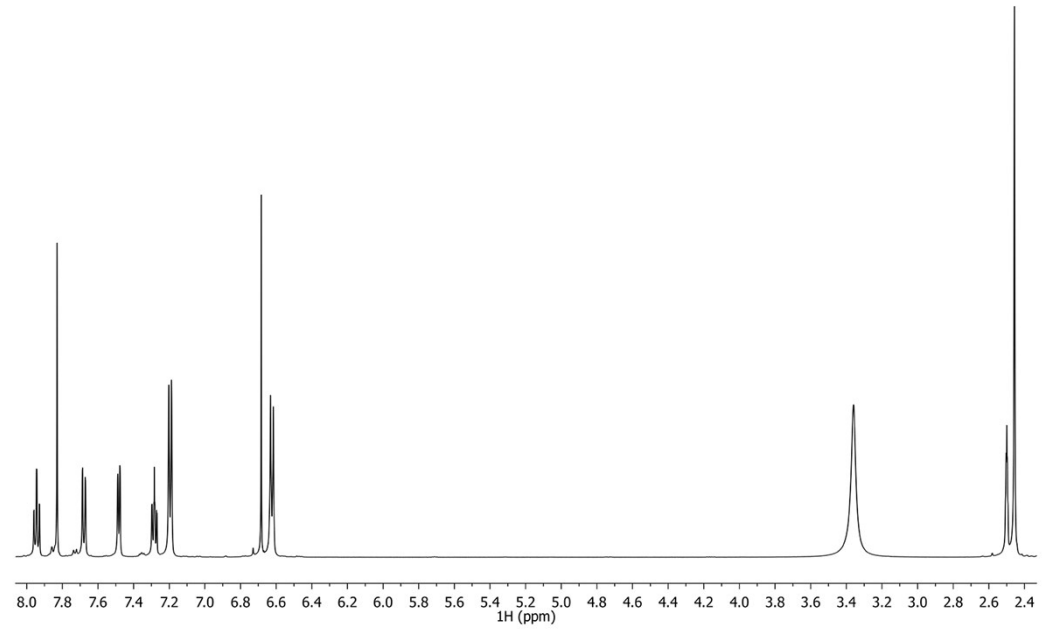

Fig. S30 ^{1}H NMR spectrum of **3-Se** in DMSO-d_6

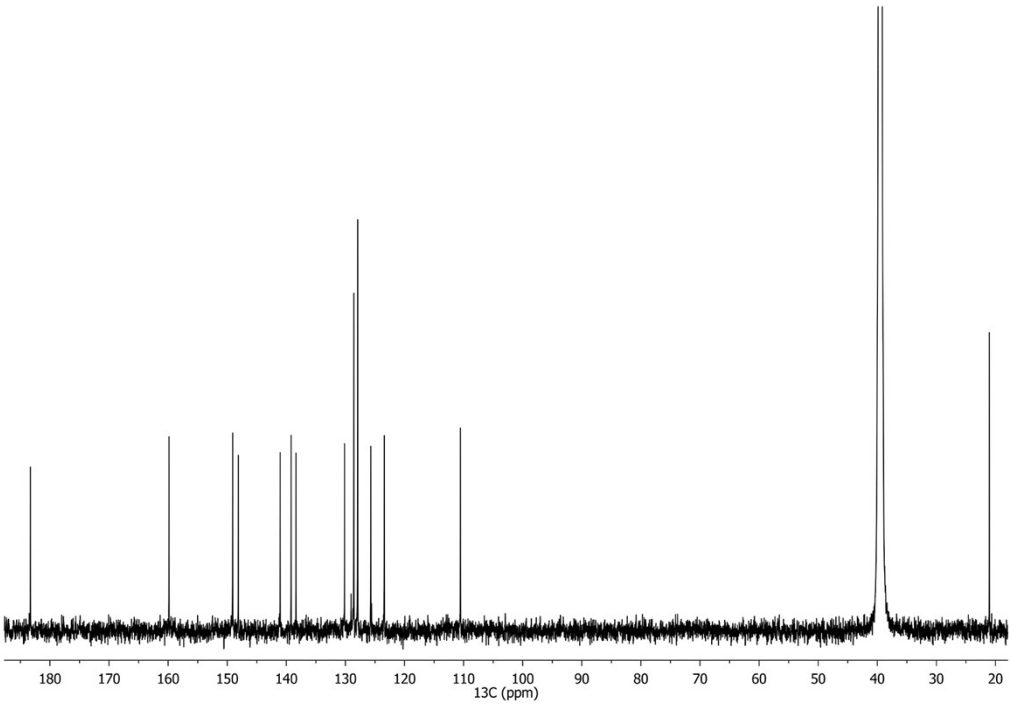

Fig. S31 ^{13}C NMR spectrum of **3-Se** in DMSO-d_6

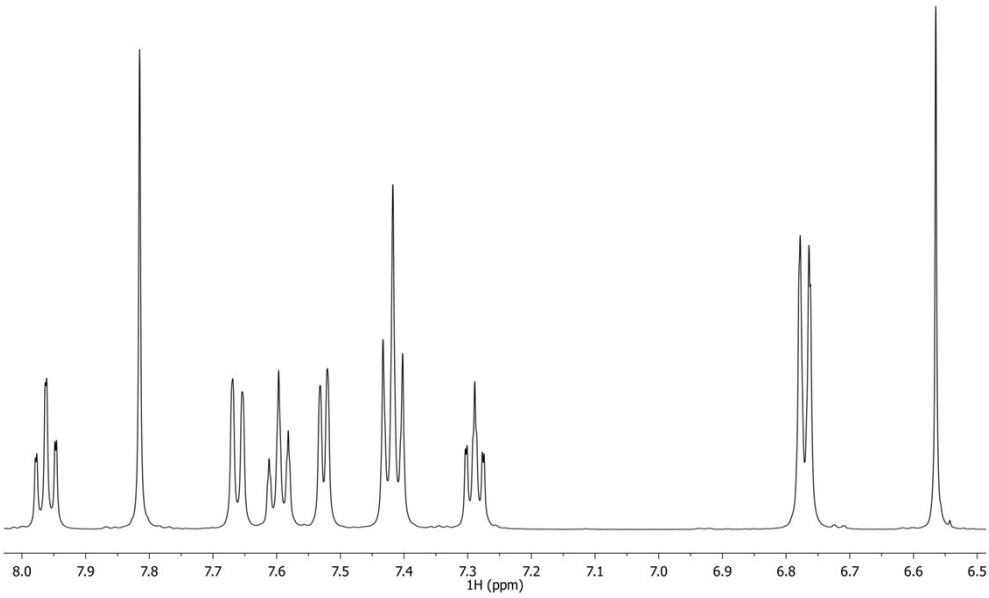

Fig. S32 ^{1}H NMR spectrum of **1-S** in DMSO-d_6

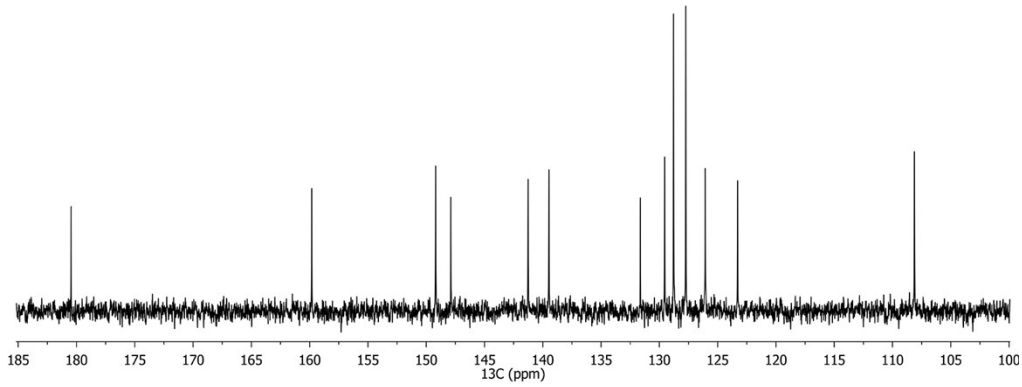

Fig. S33 ^{13}C NMR spectrum of **1-S** in DMSO-d_6

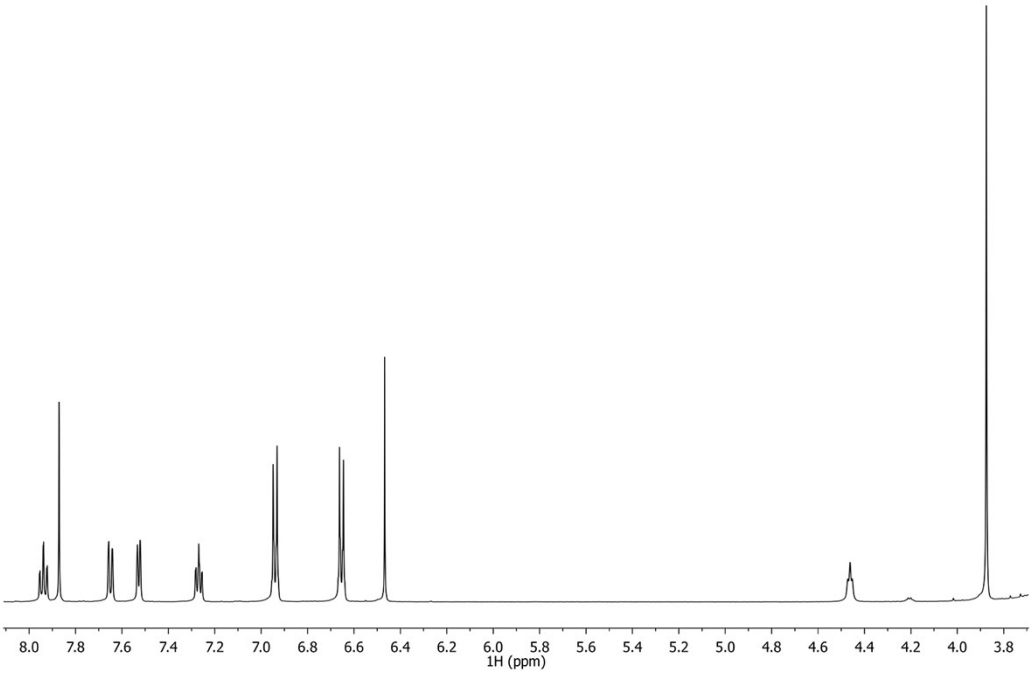

Fig. S34 ^{1}H NMR spectrum of **2-S** in DMSO-d_6

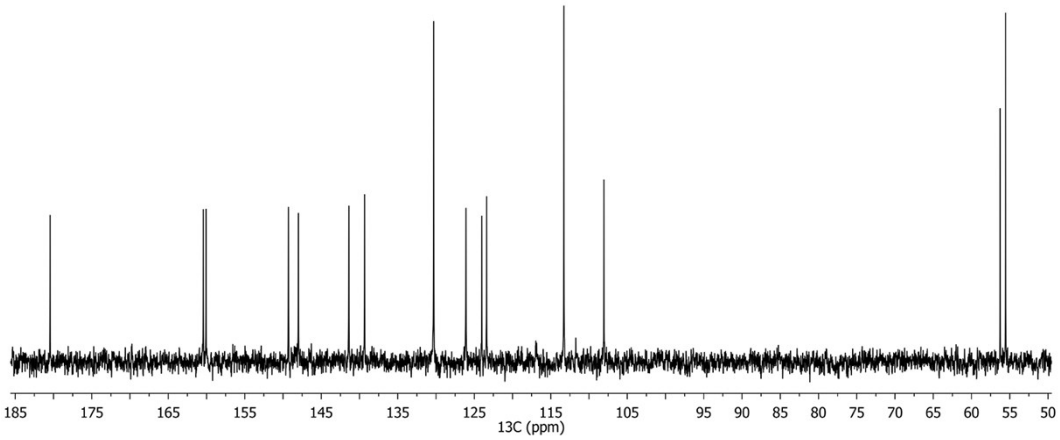

Fig. S35 ^{13}C NMR spectrum of **2-S** in DMSO-d_6

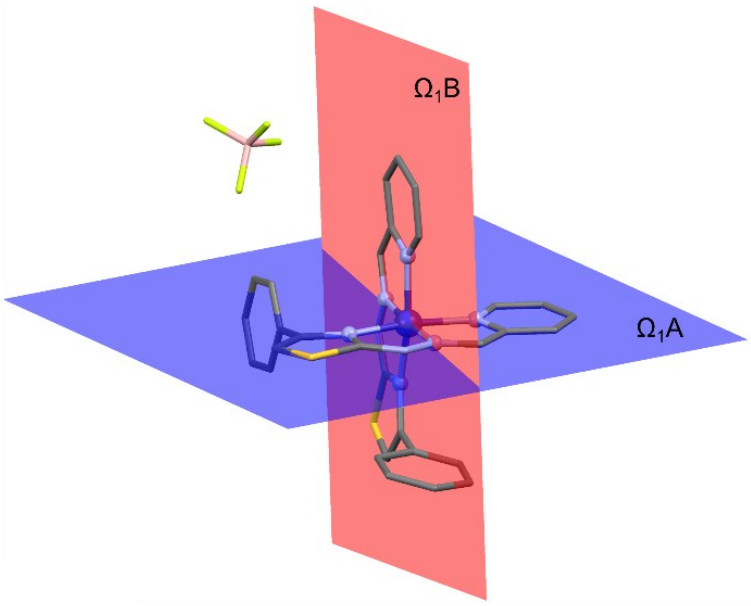

Fig. S36 Orthogonal nature of ligands coordination seen through chelate planes Ω_1A and Ω_1B.

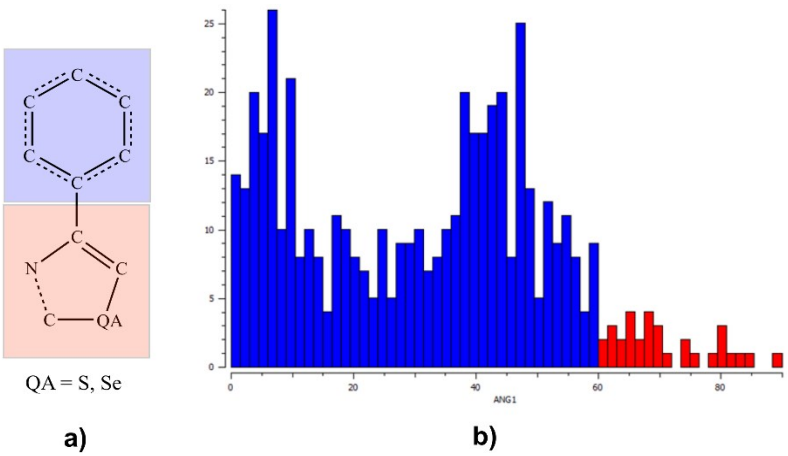

Fig. S37 (**a**) Query used in the Cambridge Structural Database (CSD) search; (**b**) Distribution of dihedral angles, 50 angles (colored in red) out of 500 hits are greater than 60°.

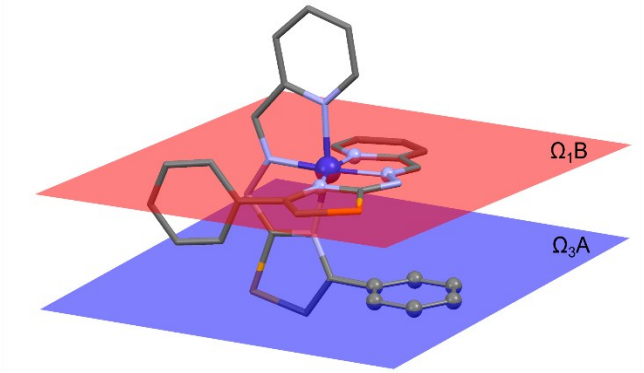

Fig. S38 Mean planes through phenyl ring of ligand A and chelate plane of ligand B.

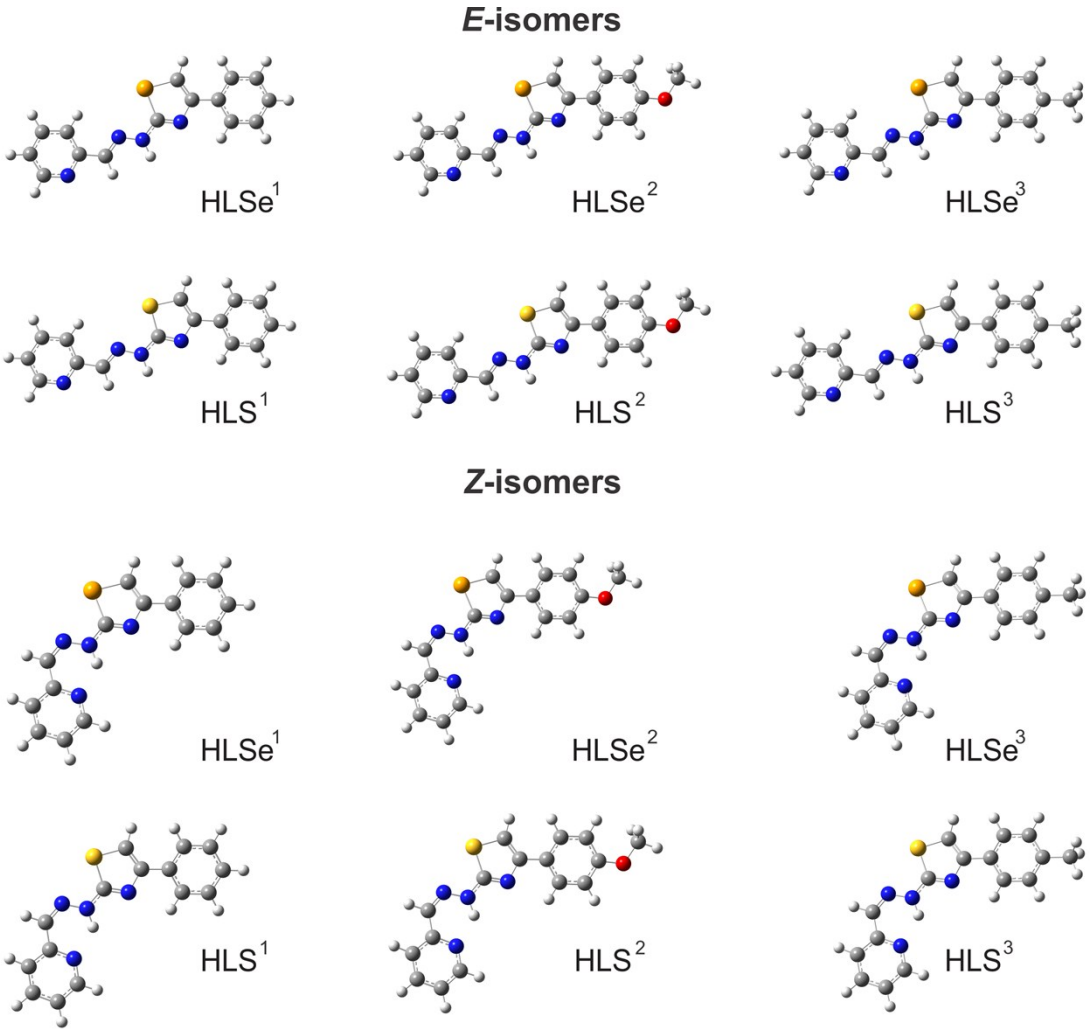

Fig. S39 DFT optimized structures of the ligands in the gas phase.

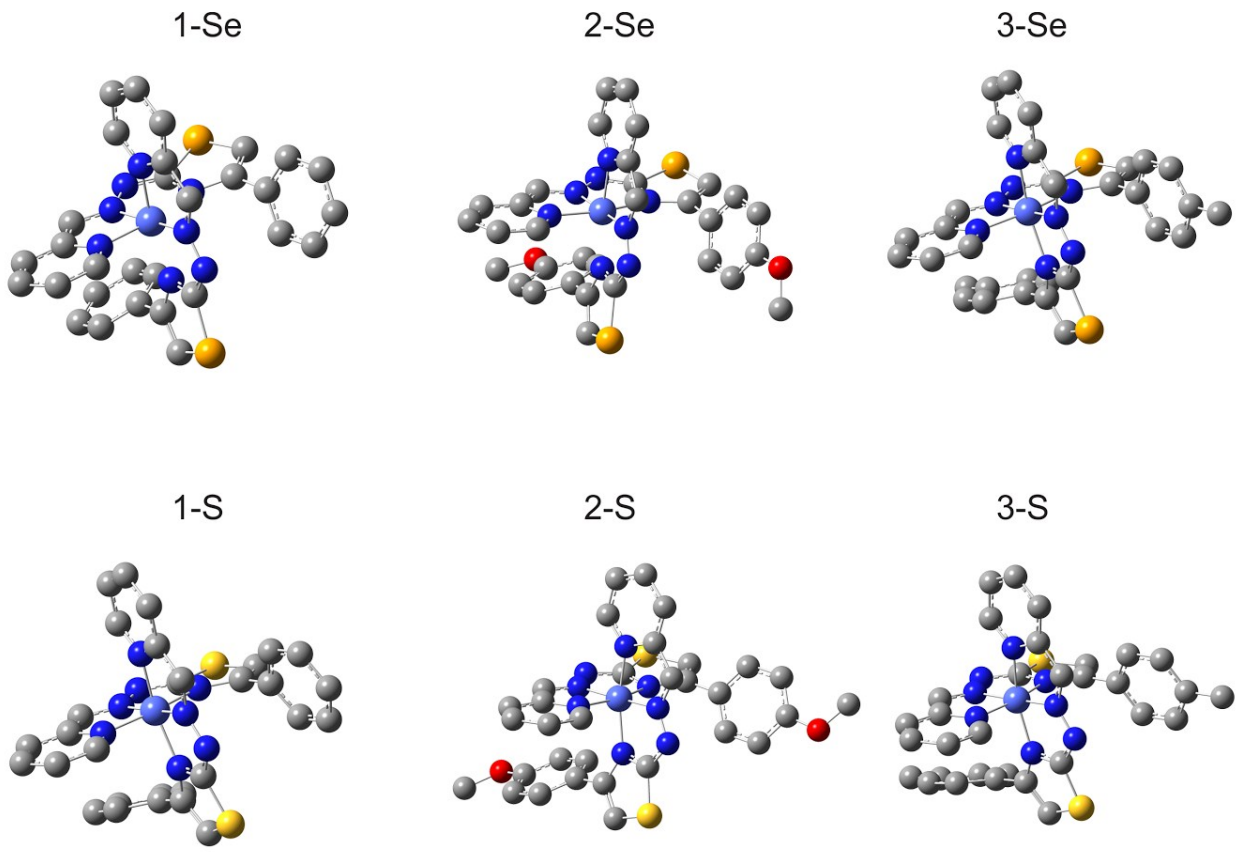

Fig. S40 DFT optimized structures of Co(III) complexes in the gas phase

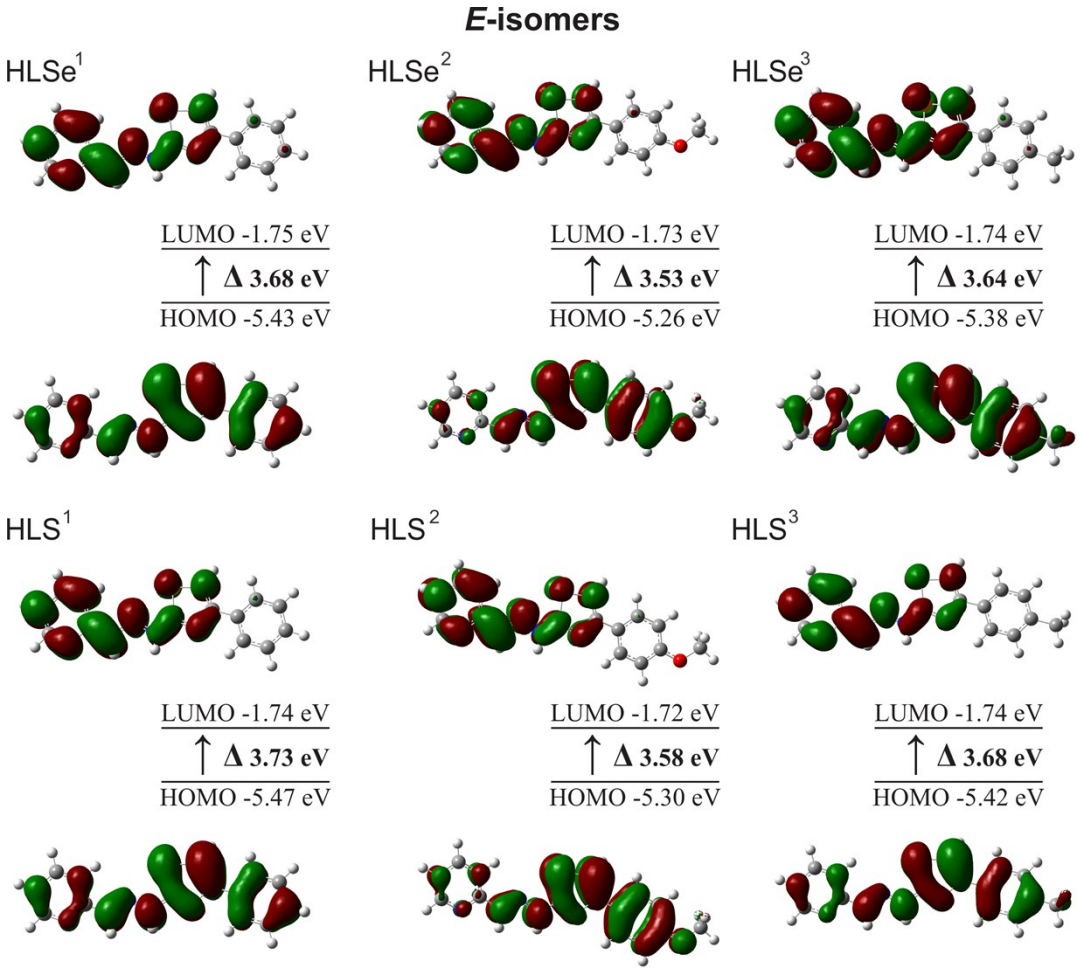

Fig. S41 Graphical representation of calculated HOMO, LUMO and HOMO-LUMO transition of *E*-1,3-thiazoles and *E*-1,3-selenazoles in DMF solvent

Table S1 Crystallographic details

	1-S	**2-S**	**1-Se**	**2-Se**	**3-Se**
Chemical formula	$C_{30}H_{22}CoN_8S_2^{+}\cdot BF_4^{-}$	$C_{32}H_{26}CoN_8O_2S_2^{+}\cdot BF_4^{-}$	$C_{30}H_{22}CoN_8Se_2^{+}\cdot BF_4^{-}$	$C_{32}H_{26}CoN_8O_2Se_2^{+}\cdot BF_4^{-}\cdot H_2O$	$C_{32}H_{26}BCoF_4N_8Se_2\cdot BF_4^{-}$
M_r	704.41	764.47	798.21	874.27	826.27
Crystal system	Tetragonal	Trigonal	Tetragonal	Triclinic	Orthorhombic
Space group	$I4_1/a$	$P3_121$	$I4_1/a$	$P\bar{1}$	$P2_12_12_1$
Temperature (K)	294	293	294	294	294
a (Å)	19.7160 (3)	9.2130 (2)	19.7293 (5),	11.1149 (3)	9.8772 (2)
b (Å)	19.7160 (3)	9.2130 (2)	19.7293 (5),	11.9728 (5)	15.1645 (4)
c (Å)	30.3333 (6)	33.5153 (7)	30.5890 (17)	13.9147 (5)	22.6936 (4)
α (°)	90	90	90, 90, 90	99.814 (3)	90
β (°)	90	90	90	96.688 (3)	90
γ (°)	90	120	90	104.417 (3)	90
V (Å^3)	11791.1 (4)	2463.63 (12)	11906.6 (9)	1742.49 (11)	3399.11 (13)
Z	16	3	16	2	4
μ (mm^{-1})	0.79	0.72	3.09	2.65	2.71
Absorption correction	Multi-scan	Multi-scan	Analytical	Analytical	Analytical
T_{min}	0.954	0.953	0.555	0.361	0.422
T_{max}	1	1	0.83	0.695	0.592
No. of measured reflections	56667	19412	17246	30249	33384
No. of independent reflections	7345	4013	6849	8296	8168
No. of observed [$I > 2\sigma(I)$] reflections	5157	3864	3835	6244	6391
R_{int}	0.050	0.028	0.059	0.029	0.029
$(\sin\theta/\lambda)_{max}$ (Å^{-1})	0.686	0.683	0.683	0.685	0.684
$R[F^2 > 2\sigma(F^2)]$	0.05	0.054	0.056	0.045	0.038
$wR(F^2)$	0.133	0.152	0.114	0.119	0.096
S	1.02	1.08	1.01	1.02	1.04
No. of reflections	7345	4013	6849	8296	8168
No. of parameters	415	232	415	499	435
No. of restraints	0	35	0	118	0
$\Delta\rho_{max}$ (e Å^{-3})	0.68	1.01	0.49	0.68	0.55
$\Delta\rho_{min}$ (e Å^{-3})	−0.45	−0.66	−0.38	−0.53	−0.37
Flack x	–	0.45 (3)	–	–	−0.015 (3)

Table S2 Voltammetric characteristics of the ligands at v = 0.10 V/s.

Ligand	E_p^R (V)	$I_p/cv^{1/2}$ [b][μA/mM(V/s)$^{1/2}$]	E_p^{Ox} (V)	$I_p/cv^{1/2}$ [μA/mM(V/s)$^{1/2}$]
HLSe[1]	–1.59	23.9	0.70	67.2
HLSe[2]	–1.60	23.0	0.65	68.8
HLSe[3]	–1.60	23.7	0.69	74.7
HLS[1]	–1.64	27.0	0.73	68.9
HLS[2]	–1.66	26.0	0.67	75.1
HLS[3]	–1.65	23.3	0.70	60.0

Table S3 Values of $k^{0'}$ for the processes I_R and II_R in solutions of complexes calculated according to reference. [S34]

Complexes	$k^{0'}$ (I_R) [a]	$k^{0'}$ (II_R)
1-S	$1.4 \cdot 10^{-4}$ ± 0.2	$1.6 \cdot 10^{-4}$ ± 0.5
2-S	$1.6 \cdot 10^{-4}$ ± 0.3	$1.7 \cdot 10^{-4}$ ± 0.5
3-S	$1.4 \cdot 10^{-4}$ ± 0.2	$1.5 \cdot 10^{-4}$ ± 0.2
1-Se	$2.0 \cdot 10^{-4}$ ± 0.3	$1.5 \cdot 10^{-4}$ ± 0.2
2-Se	$1.6 \cdot 10^{-4}$ ± 0.4	$1.6 \cdot 10^{-4}$ ± 0.2
3-Se	$1.6 \cdot 10^{-4}$ ± 0.4	$1.8 \cdot 10^{-4}$ ± 0.4

[a] In m/s.

Table S4 Elements of DFT optimized geometries of *E*- and *Z*-isomers of ligands compared with available crystal structure data.

Compound, X=S	**HLS[1]***	**HLS[2]***	**HLS[3]***	**HLS[1]***	**HLS[2]***	**HLS[3]***
			E-isomer			Z-isomer
Bond (Å)						
N_4–C_7	1.289	1.289	1.298 (1.300)[a]	1.299	1.300	1.299 (1.265)[b]
N_4–C_9	1.389	1.390	1.389 (1.388)[a]	1.388	1.388	1.388 (1.373)[b]
X_1–C_7	1.759	1.758	1.758 (1.738)[a]	1.762	1.761	1.762 (1.700)[b]
X_1–C_8	1.746	1.747	1.746 (1.723)[a]	1.744	1.746	1.745 (1.690)[b]
C_1–C_6	1.465	1.465	1.465 (1.465)[a]	1.462	1.462	1.462 (1.414)[b]
C_6–N_2	1.287	1.288	1.288 (1.277)[a]	1.298	1.298	1.298 (1.260)[b]
N_2–N_3	1.344	1.343	1.344 (1.360)[a]	1.337	1.336	1.337 (1.337)[b]
N_3–H	1.019	1.019	1.019 (0.872)[a]	1.026	1.026	1.026 (0.860)[b]
Angle (°)						
C_7–N_4–C_9	110.77	110.85	110.80 (109.98)[a]	110.84	110.84	110.84 (109.82)[b]
C_7–X_1–C_8	87.33	87.35	87.37 (87.87)[a]	87.35	87.35	87.35 (87.76)[b]
Torsion (°)						
X_1–C_8–C_9–C_{10}	179.90	180.00	180.00 (178.83)[a]	179.89	179.93	179.89 (178.21)[b]
N_4–C_9–C_{10}–C_{11}	2.07	2.82	–0.74 (–12.51)[a]	5.98	5.59	4.86 (4.46)[b]
X_1–C_7–N_3–N_2	–0.13	–0.10	–0.07 (–0.85)[a]	0.21	0.29	0.04 (4.69)[b]
N_1–C_1–C_6–N_2	179.98	179.88	179.98 (–175.82)[a]	–0.33	–0.21	–0.30 (3.75)[b]
C_1–C_6–N_2–N_3	179.94	179.96	179.90 (179.93)[a]	0.13	0.05	0.21 (–0.25)[b]

Table S4 (continued).

Compound, X=Se	**HLSe[1]***	**HLSe[2]***	**HLSe[3]***	**HLSe[1]***	**HLSe[2]***	**HLSe[3]***
			E-isomer			Z-isomer
Bond (Å)						
N_4–C_7	1.293	1.293	1.292	1.293	1.294	1.294
N_4–C_9	1.391	1.392	1.392	1.390	1.390	1.390
X_{11}–C_7	1.890	1.888	1.890	1.893	1.893	1.892
X_{11}–C_8	1.876	1.877	1.877	1.875	1.875	1.875
C_1–C_6	1.465	1.465	1.465	1.462	1.462	1.462
C_6–N_2	1.287	1.287	1.287	1.298	1.298	1.298
N_2–N_3	1.344	1.343	1.343	1.337	1.336	1.337
N_3–H	1.019	1.019	1.019	1.027	1.026	1.026
Angle (°)						
C_7–N_4–C_9	112.75	112.78	112.78	112.88	112.95	112.84
C_7–X_1–C_8	83.19	83.20	83.16	83.20	83.22	83.23
Torsion (°)						
X_1–C_8–C_9–C_{10}	–179.99	–179.90	–179.94	179.90	179.96	179.86
N_4–C_9–C_{10}–C_{11}	–1.02	5.15	0.24	6.78	6.37	6.25
X_1–C_7–N_3–N_2	–0.01	0.00	–0.08	0.17	0.15	0.18
N_1–C_1–C_6–N_2	–179.88	–180.00	179.94	–0.20	–0.23	–0.25
C_1–C_6–N_2–N_3	–179.98	–179.99	179.98	0.09	0.14	0.14

* Optimized geometries obtained by the use of DFT calculations with the B3LYP/6-31G(d) basis set

[a] Crystal structure data obtained from X-ray diffraction analysis in the present work

[b] Crystal structure data taken from literature[S35]

Table S5 Calculated the relative energy Δ*E* (kcal/mol) of *E*-1,3-thiazoles and *E*-1,3-selenazoles).

Compound, X=S	*E*-**HLS**[1]	*Z*-**HLS**[1]	*E*-**HLS**[2]	*Z*-**HLS**[2]	*E*-**HLS**[3]	*Z*-**HLS**[3]
ΔE (kcal/mol)	2.630 [a]	0.000 [a]	2.571 [a]	0.000 [a]	2.615 [a]	0.000 [a]
	2.212 [b]	0.000 [b]	2.184 [b]	0.000 [b]	2.253 [b]	0.000 [b]

Compound, X=Se	*E*-**HLSe**[1]	*Z*-**HLSe**[1]	*E*-**HLSe**[2]	*Z*-**HLSe**[2]	*E*-**HLSe**[3]	*Z*-**HLSe**[3]
ΔE (kcal/mol)	2.574 [a]	0.000 [a]	2.529 [a]	0.000 [a]	2.496 [a]	0.000 [a]
	2.057 [b]	0.000 [b]	2.053 [b]	0.000 [b]	2.044 [b]	0.000 [b]

DFT/ B3LYP/6-31G(d) calculated the relative energy *E*, defined as zero-point corrected total energy and with respect to more stable isomeric form.[a] In the gas phase; [b] In DMF solvent.

Table S6 Comparison of average values of the theoretically calculated Co–N bond lengths (in Å) and N–Co–N angles (in °) obtained for the complex **1-S**, using two DFT functionals with several basis sets and experimental measured values.

functionals / basis sets	$Co–N_1$	$Co–N_2$	$Co–N_4$	N–Co–N	
				trans	*cis*
b3lyp / 6-31g(d,p) [a] / 6-31g(d)[a]	1.966	1.899	1.976	167.83	90.38
b3lyp / 6-31g(2d,2p) [b] / 6-31g(d,p) [b] / 6-31g(d)[b]	1.966	1.899	1.977	167.83	90.38
b3lyp/ LanL2DZ-epc [c] / 6-31g(d) [c]	1.977	1.909	1.992	167.83	90.38
bvp86 / 6-31g(d,p)[d] / 6-31g(d) [d]	1.944	1.888	1.958	168.02	90.37
bvp86 / LanL2DZ-epc[e] / 6-31g(d)[e]	1.960	1.902	1.981	168.08	90.37
bvp86 / cc-pVTZ[f] / 6-31g(d)[f]	1.958	1.900	1.973	167.67	90.39
measured[g]	1.947	1.887	1.946	167.17	90.41

[a] B3LYP functional with 6-31g(d,p) on Co and 6-31g(d) on all others atoms

[b] B3LYP functional with 6-31g(2d,2p) on Co, 6-31g(d,p) on N atoms and 6-31g(d) on all others atoms

[c] B3LYP functional with LanL2DZ-epc on Co and 6-31g(d) on all others atoms

[d] BVP86 functional with 6-31g(d,p) on Co and 6-31g(d) on all others atoms

[e] BVP86 functional with LanL2DZ-epc on Co and 6-31g(d) on all others atoms

[f] BVP86 functional with cc-pVTZ on Co and 6-31g(d) on all others atoms

[g] Experimental Co-N bond lengths

Table S7 Comparison of average values of the experimental and theoretical calculated Co–N bond lengths (in Å) and N–Co–N angles (in °) obtained for the **(1–3)-Se** and **(1–3)-S** complexes

Compound		**1-Se**[*]	**2-Se**[*]	**3-Se**[*]
Bond (Å)				
$Co–N_1$		1.946 (1.949)[a]	1.945 (1.953)[a]	1.947 (1.948)[a]
$Co–N_2$		1.884 (1.883)[a]	1.884 (1.888)[a]	1.886 (1.888)[a]
$Co–N_4$		1.973 (1.955)[a]	1.971 (1.957)[a]	1.960 (1.950)[a]
Angle (°)				
N–Co–N	*trans*	168.10 (166.97)[a]	168.13 (166.58)[a]	167.75 (167.05)[a]
	cis	90.40 (90.42)[a]	90.35 (90.42)[a]	90.37 (90.42)[a]

Compound		**1-S**[*]	**2-S**[*]	**3-S**[*]
Bond (Å)				
$Co–N_1$		1.944 (1.944)[a]	1.944 (1.948)[a]	1.944 (1.946)[b]
$Co–N_2$		1.888 (1.887)[a]	1.887 (1.886)[a]	1.889 (1.888)[a]
$Co–N_4$		1.958 (1.946)[a]	1.967 (1.948)[a]	1.956 (1.943)[a]
Angle (°)				
N–Co–N	*trans*	168.02 (167.17)[a]	168.27 (-)[a]	167.89 (167.33)[a]
	cis	90.37 (90.41)[a]	90.39 (-)[a]	90.37 (90.41)[a]

[*] Optimized geometries obtained by the use of DFT calculations with the B3LYP/6-31G(d) basis set

[a] Crystal structure data obtained from X-ray diffraction analysis in the present work

[b] Reference S20

Table S8 Average values of experimental and calculated chemical shifs (δ in ppm), coupling constants (J in Hz) and assignments of the signals in ^{1}H and ^{13}C NMR spectra of **(1–3)-Se** and **(1–3)-S** complexes

1-S

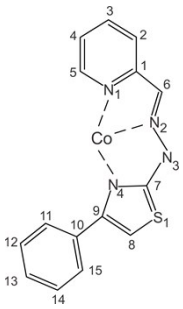

	^{1}H				^{13}C		
	Exp.	Calc.	Calc.^{scaled}		Exp.	Calc.	Calc.^{scaled}
$H–C_8$	6.56 (s, 1H)	6.12	6.60	C_8	108.12	114.46	106.39
$H–C_{11,15}$	6.77 (d, 2H, ^{3}J = 6.9)	7.14	6.81	C_2	123.28	118.82	121.24
$H–C_{13}$	7.29 (ddd, 1H, ^{3}J = 7.3, ^{3}J = 6.1, ^{3}J = 1.3)	7.76	7.31	C_4	126.06	120.78	123.97
$H–C_{12,14}$	7.42 (t, 2H, ^{3}J = 7.7)	7.63	7.44	$C_{11,15}$	127.73	126.13	125.61
$H–C_5$	7.53 (d, 1H, ^{3}J = 5.6)	8.18	7.54	$C_{12,14}$	128.78	123.11	126.63
$H–C_4$	7.60 (t, 1H, ^{3}J = 7.5)	7.16	7.61	C_{10}	129.54	127.68	127.38
$H–C_2$	7.66 (d, 1H, ^{3}J = 7.4)	7.55	7.67	C_{13}	131.63	125.18	129.43
$H–C_6$	7.82 (s, 1H)	8.15	7.83	C_6	139.47	134.94	137.11
$H–C_3$	7.96 (td, 1H, ^{3}J = 7.8, ^{3}J = 1.2)	7.87	7.96	C_3	141.27	136.65	138.87
				C_9	147.89	147.56	145.36
				C_5	149.19	146.47	146.64
				C_1	159.81	154.59	157.04
				C_7	180.47	179.14	177.29

Table S8 (continued)

1-Se

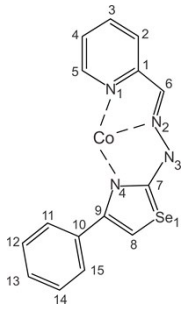

	^{1}H				^{13}C		
	Exp.	Calc.	Calc.^{scaled}		Exp.	Calc.	Calc.^{scaled}
H–C_8	6.75 (s, 1H)	6.33	6.79	C_8	110.90	118.78	109.11
H–$C_{11,15}$	6.75 (d, 2H, ^{3}J = 6.4)	7.27	6.79	C_2	123.68	119.27	121.64
H–C_{13}	7.29 (ddd, 1H, ^{3}J = 7.4, ^{3}J = 5.9, ^{3}J = 1.4)	7.75	7.31	C_4	125.99	120.80	123.90
H–$C_{12,14}$	7.40 (t, 2H, ^{3}J = 7.8)	7.65	7.42	$C_{11,15}$	127.66	125.69	125.54
H–C_5	7.49 (d, 1H, ^{3}J = 5.3)	8.07	7.51	$C_{12,14}$	128.89	123.46	126.74
H–C_4	7.58 (ddd, 1H, ^{3}J = 7.5, ^{3}J = 6.4, ^{3}J = 1.2)	7.08	7.59	C_{10}	129.30	129.71	127.14
H–C_2	7.68 (dd, 1H, ^{3}J = 8.0, ^{3}J = 0.8)	7.33	7.69	C_{13}	133.13	124.65	130.90
H–C_6	7.82 (s, 1H)	7.87	7.83	C_6	139.52	134.13	137.16
H–C_3	7.95 (td, 1H, ^{3}J = 7.7, ^{3}J = 1.3)	7.76	7.95	C_3	141.26	136.29	138.86
				C_9	148.22	148.26	145.69
				C_5	149.33	146.17	146.77
				C_1	159.94	154.17	157.17
				C_7	183.60	186.75	180.36

Table S8 (continued)

2-S

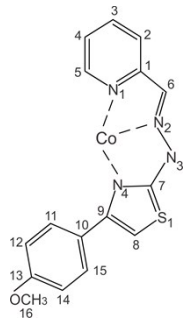

	^{1}H				^{13}C		
	Exp.	Calc.	Calc.^{scaled}		Exp.	Calc.	Calc.^{scaled}
H–C_{16}	3.23 (s, 3H)	4.11	-	C_{16}	55.55	55.05	-
H–C_8	6.47 (s, 1H)	6.15	6.52	C_8	108.06	113.97	106.33
H–$C_{11,15}$	6.65 (d, 2H, ^3J = 8.6)	7.16	6.69	C_2	123.39	118.78	121.35
H–$C_{12,14}$	6.94 (d, 2H, ^3J = 8.6)	6.94	6.97	C_4	126.08	120.81	123.99
H–C_4	7.27 (ddd, 1H, ^3J = 7.3, ^3J = 6.1, ^3J = 1.3)	7.08	7.29	$C_{12,14}$	113.29	109.28	111.45
H–C_5	7.53 (d, 1H, ^3J = 5.6)	8.08	7.54	$C_{11,15}$	130.30	127.12	128.12
H–C_2	7.65 (d, 1H, ^3J = 7.9)	7.28	7.66	C_{10}	124.01	120.45	121.96
H–C_6	7.87 (s, 1H)	7.92	7.87	C_{13}	160.42	154.37	157.64
H–C_3	7.94 (td, 1H, ^3J = 7.8, ^3J = 1.2)	7.76	7.94	C_6	139.33	133.99	136.97
				C_3	141.39	136.34	138.99
				C_9	147.98	148.03	145.45
				C_5	149.29	145.89	146.73
				C_1	160.06	154.09	157.29
				C_7	180.45	179.63	177.27

Table S8 (continued)

2-Se		^{1}H				^{13}C		
		Exp.	Calc.	Calc.^{scaled}		Exp.	Calc.	Calc.^{scaled}
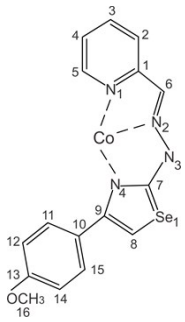	H–C_{16}	3.89 (s, 3H),	4.13	-	C_{16}	55.28	55.10	-
	H–C_{8}	6.69 (s, 1H)	6.27	6.73	C_{8}	110.57	118.25	108.79
	H–$C_{11,15}$	6.65 (d, 2H, ^{3}J = 8.4)	7.17	6.69	C_{2}	123.49	119.12	121.45
	H–$C_{12,14}$	6.93 (d, 2H, ^{3}J = 8.6)	6.94	6.96	C_{4}	125.77	120.66	123.68
	H–C_{4}	7.29 (ddd, 1H, ^{3}J = 7.2, ^{3}J = 6.1, ^{3}J = 0.9)	7.06	7.31	$C_{12,14}$	112.90	109.15	111.07
	H–C_{5}	7.50 (d, 1H, ^{3}J = 5.7)	8.07	7.52	$C_{11,15}$	130.08	127.41	127.91
	H–C_{2}	7.69 (d, 1H, ^{3}J = 7.7)	7.32	7.70	C_{10}	125.29	121.63	123.21
	H–C_{6}	7.90 (s, 1H)	7.90	7.90	C_{13}	159.94	154.30	157.17
	H–C_{3}	7.95 (td, 1H, ^{3}J = 7.9, ^{3}J = 0.8)	7.76	7.95	C_{6}	139.11	133.74	136.76
					C_{3}	141.09	136.20	138.70
					C_{9}	147.97	148.19	145.44
					C_{5}	149.17	146.17	146.62
					C_{1}	159.94	154.24	157.17
					C_{7}	183.19	186.37	179.96

Table S8 (continued)

3-S		^{1}H				^{13}C		
		Exp.	Calc.	Calc.^{scaled}		Exp.	Calc.	Calc.^{scaled}
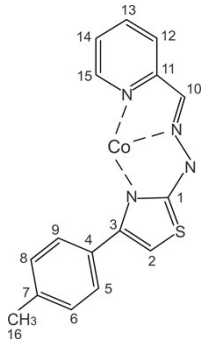	H–C_{16}	2.46 (s, 3H)	2.67	-	C_{16}	21.19	23.26	-
	H–C_8	6.50 (s, 1H)	6.10	6.55	C_8	107.98	113.93	106.25
	H–$C_{11,15}$	6.64 (d, 2H, ^3J = 8.0)	7.06	6.68	C_2	123.22	118.83	121.19
	H–$C_{12,14}$	7.21 (d, 2H, ^3J = 8.0)	7.45	7.23	C_4	125.98	120.68	123.89
	H–C_4	7.28 (ddd, 1H, ^3J = 7.4 , ^3J = 5.7, ^3J = 1.4)	7.17	7.30	$C_{12,14}$	128.22	123.95	126.09
	H–C_5	7.52 (d, 1H, ^3J = 5.4)	8.19	7.53	$C_{11,15}$	128.66	125.96	126.52
	H–C_2	7.65 (dd, 1H, ^3J = 8.0, ^3J = 0.8)	7.55	7.66	C_{10}	128.84	124.95	126.69
	H–C_6	7.82 (s, 1H)	8.19	7.83	C_{13}	138.90	136.82	136.55
	H–C_3	7.99 (td, 1H, J = 7.8, ^3J = 1.3)	7.86	7.99	C_6	139.35	134.75	136.99
					C_3	141.01	136.48	138.62
					C_9	148.01	147.58	145.48
					C_5	149.12	146.50	146.57
					C_1	159.91	154.65	157.14
					C_7	180.43	179.11	177.25

Table S8 (continued)

3-Se		^{1}H				^{13}C		
		Exp.	Calc.	Calc.^{scaled}		Exp.	Calc.	Calc.^{scaled}
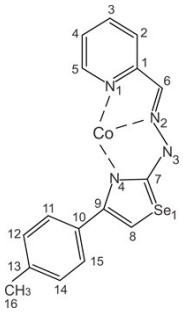	H–C_{16}	2.46 (s, 3H)	2.68	-	C_{16}	21.05	23.17	-
	H–$C_{11,15}$	6.62 (d, 2H, ^3J = 7.7)	7.05	6.66	C_8	110.54	118.41	108.76
	H–C_8	6.68 (s, 1H)	6.24	6.72	C_2	123.42	118.82	121.38
	H–$C_{12,14}$	7.19 (d, 2H,^3J = 7.6)	7.44	7.21	C_4	125.71	120.63	123.63
	H–C_4	7.28 (ddd, 1H, ^3J = 7.4, ^3J = 5.9, ^3J = 1.4)	7.14	7.30	$C_{12,14}$	127.92	123.74	125.79
	H–C_5	7.48 (d, 1H, ^3J = 5.5)	8.13	7.50	$C_{11,15}$	128.59	126.54	126.45
	H–C_2	7.68 (dd, 1H, $^3J_{14,15}$ = 7.9, ^3J = 0.6)	7.53	7.69	C_{10}	130.16	126.11	127.99
	H–C_6	7.83 (s, 1H)	8.08	7.84	C_{13}	138.36	136.43	136.02
	H–C_3	7.94 (td, 1H, ^3J = 7.8, ^3J = 1.3)	7.83	7.94	C_6	139.19	134.51	136.84
					C_3	141.05	136.38	138.66
					C_9	148.12	147.51	145.59
					C_5	149.07	146.51	146.52
					C_1	159.85	154.56	157.08
					C_7	183.31	185.69	180.07

Exp. - Experimental 1H and 13C NMR chemical shifts. Calc. - Calculated ^{1}H and ^{13}C NMR chemical shifts at PCM(DMSO)DFT/B3LYP/6-31G(d,p)/6-31G(d) level of theory with respect to TMS. Calculated chemical shifts of TMS at PCM(DMSO)DFT/B3LYP/6-31G(d) have values 190.11 ppm for ^{13}C and 32.17 ppm for 1H. Calc.scaled - the linearly scaled calculated values (Calc.) by applied the correlation between the experimental and the calculated (Calc.) chemical shifts. Linear Regression was applied at experimental and calculated chemical shifts of all C-sp^2 atoms and the best fit straight line corresponding to δcalc.= 0.43 + 0.98δ exp. (R=0.98). Resulting linear regression line for all protons attached to C-sp^2 atoms has form δcalc.= 0.24 + 0.97δ exp. (R=0.79).

Table S9 TD-DFT/B3LYP calculated electronic transitions (absorption maxima λ_{max} in cm^{-1} and nm), oscillator strengths (*f*) and major MO contributors in percent of *E*-1,3-thiazoles and *E*-1,3-selenazoles in DMF solvent.

Compound	No.	λ_{max}		*f*	MO major contributors					
					Transition	%	Transition	%	Transition	%
HLSe[1]	1	**26409**	**379**	0.4185	HOMO→LUMO	98				
	2	33331	300	0.0336	H-1→LUMO	29	HOMO→L+1	67		
	3	34349	291	0.3009	H-1→LUMO	18	HOMO→L+1	10	HOMO→L+2	68
	4	**34721**	**288**	0.7809	H-1→LUMO	49	HOMO→L+1	20	HOMO→L+2	28
	5	35498	282	0.0012	HOMO→L+4	97				
	6	35791	279	0.0011	H-3→LUMO	96	H-3→L+1	2		
	7	37511	267	0.0180	H-2→LUMO	36	H-2→L+1	10	HOMO→L+3	48
	8	38554	259	0.0033	H-2→LUMO	61	HOMO→L+3	30	H-1→L+1	5
	9	40536	247	0.0010	H-4→LUMO	48	H-1→L+2	11	HOMO→L+5	21
	10	40855	245	0.0003	H-6→LUMO	93	H-6→L+1	4	H-6→L+5	2
	11	**41080**	**243**	0.1792	H-4→LUMO	14	H-1→L+1	74	HOMO→L+3	4
	12	41508	241	0.0124	H-5→LUMO	14	H-1→L+2	39	HOMO→L+5	20
	13	42081	238	0.0553	H-5→LUMO	76	HOMO→L+5	15	H-1→L+2	3
	14	42358	236	0.0031	H-3→L+2	98				
	15	42894	233	0.0078	H-2→L+1	45	H-1→L+3	16	HOMO→L+3	14

Table S9 (continued)

Compound	No.	λ_{max}		*f*	MO major contributors					
					Transition	%	Transition	%	Transition	%
HLSe²	1	**25265**	**396**	0.2651	HOMO→LUMO	99				
	2	31939	313	0.7786	H-1→LUMO	97				
	3	33518	298	0.0635	HOMO→L+1	51	HOMO→L+2	45		
	4	**33937**	**295**	0.3403	HOMO→L+1	43	HOMO→L+2	50		
	5	34772	288	0.0012	HOMO→L+3	16	HOMO→L+4	80		
	6	35844	279	0.0011	H-4→LUMO	97	H-4→L+1	2		
	7	36815	272	0.0776	HOMO→L+3	65	HOMO→L+4	13		
	8	38740	258	0.0838	H-2→LUMO	87	H-3→LUMO	3	HOMO→L+3	5
	9	39271	255	0.1111	H-1→L+1	78	H-7→LUMO	3	HOMO→L+5	8
	10	**39317**	**254**	0.1567	H-3→LUMO	44	H-1→L+2	39	H-7→LUMO	5
	11	40076	250	0.0651	H-3→LUMO	31	H-1→L+2	37	HOMO→L+5	24
	12	40818	245	0.0042	H-6→LUMO	74	H-5→LUMO	14	HOMO→L+5	5
	13	40864	245	0.0173	H-6→LUMO	20	H-5→LUMO	55	HOMO→L+5	11
	14	42371	236	0.0047	H-4→L+1	18	H-4→L+2	79		
	15	42382	236	0.1043	H-5→LUMO	20	H-1→L+2	11	HOMO→L+5	36

Table S9 (continued)

Compound	No.	λ_{max}		*f*	MO major contributors					
					Transition	%	Transition	%	Transition	%
HLSe[3]	1	**26090**	**383**	0.3747	HOMO→LUMO	99				
	2	33211	301	0.2759	H-1→LUMO	72	HOMO→L+1	25		
	3	34055	294	0.4179	H-1→LUMO	10	HOMO→L+1	41	HOMO→L+2	45
	4	**34382**	**291**	0.5260	H-1→LUMO	15	HOMO→L+1	31	HOMO→L+2	51
	5	35311	283	0.0002	HOMO→L+4	98				
	6	35855	279	0.0011	H-3→LUMO	96	H-3→L+1	2		
	7	37186	269	0.0184	H-2→LUMO	31	H-2→L+1	10	HOMO→L+3	54
	8	38227	262	0.0034	H-2→LUMO	67	HOMO→L+3	25	H-1→L+1	5
	9	40268	248	0.0031	H-4→LUMO	28	H-1→L+2	19	HOMO→L+5	17
	10	**40620**	**246**	0.2442	H-4→LUMO	20	H-1→L+1	65		
	11	40837	245	0.0001	H-6→LUMO	93	H-6→L+1	3	H-6→L+5	2
	12	41150	243	0.0228	H-5→LUMO	24	H-1→L+2	31	HOMO→L+5	25
	13	41374	242	0.0370	H-5→LUMO	67	H-4→LUMO	13		
	14	42404	236	0.0030	H-3→L+2	97				
	15	42714	234	0.0184	H-4→LUMO	14	H-2→L+1	33	H-1→L+3	15

Table S9 (continued)

Compound	No.	λ_{max}		*f*	MO major contributors					
					Transition	%	Transition	%	Transition	%
HLS[1]	1	**26929**	**371**	0.5163	HOMO→LUMO	98				
	2	33732	296	0.0289	H-1→LUMO	28	HOMO→L+1	69		
	3	34672	288	0.1744	H-1→LUMO	12	HOMO→L+2	77	HOMO→L+1	6
	4	**35120**	**285**	0.7943	H-1→LUMO	57	HOMO→L+1	22	HOMO→L+2	18
	5	35771	280	0.0011	H-3→LUMO	97				
	6	37773	265	0.0125	H-2→LUMO	34	H-2→L+1	11	HOMO→L+3	50
	7	38737	258	0.0027	H-2→LUMO	64	HOMO→L+3	28	H-1→L+1	4
	8	39026	256	0.0000	HOMO→L+5	98				
	9	40905	244	0.0001	H-4→LUMO	52	H-1→L+2	14	HOMO→L+4	16
	10	**41596**	**240**	0.2430	H-1→L+1	82	H-4→LUMO	8	HOMO→L+3	3
	11	42015	238	0.0178	H-6→LUMO	15	H-1→L+2	36	HOMO→L+4	30
	12	42379	236	0.0030	H-3→L+2	97				
	13	42522	235	0.0000	H-5→LUMO	92	H-5→L+1	3	H-5→L+4	2
	14	42961	233	0.0088	H-2→L+1	44	H-1→L+3	19	HOMO→L+3	15
	15	43833	228	0.0010	H-8→LUMO	96				

Table S9 (continued)

Compound	No.	λ_{max}		*f*	MO major contributors					
					Transition	%	Transition	%	Transition	%
HLS²	1	**25753**	**388**	0.3256	HOMO→LUMO	99				
	2	32179	311	0.7855	H-1→LUMO	97				
	3	33823	296	0.0235	HOMO→L+1	39	HOMO→L+2	56		
	4	**34343**	**291**	0.3198	HOMO→L+1	54	HOMO→L+2	38		
	5	35859	279	0.0011	H-4→LUMO	97	H-4→L+1	2		
	6	36989	270	0.0837	HOMO→L+3	77	H-2→LUMO	5	H-2→L+1	7
	7	38315	261	0.0000	HOMO→L+5	97				
	8	39135	256	0.0100	H-2→LUMO	87	H-1→L+1	8	HOMO→L+3	3
	9	39499	253	0.0018	H-3→LUMO	14	H-1→L+1	33	H-1→L+2	26
	10	**39653**	**252**	0.3091	H-3→LUMO	19	H-1→L+1	43	H-1→L+2	24
	11	40442	247	0.0881	H-3→LUMO	36	H-1→L+2	28	HOMO→L+4	31
	12	42342	236	0.0030	H-4→L+1	19	H-4→L+2	78		
	13	42448	236	0.0637	H-3→LUMO	16	H-1→L+3	18	HOMO→L+4	33
	14	42458	236	0.0016	H-6→LUMO	90	H-6→L+1	3	H-6→L+4	2
	15	42935	233	0.0362	H-2→L+1	10	H-1→L+3	49	HOMO→L+4	20

Table S9 (continued)

Compound	No.	λ_{max}		*f*	MO major contributors					
					Transition	%	Transition	%	Transition	%
HLS³	1	**26561**	**376**	0.4682	HOMO→LUMO	99				
	2	33538	298	0.3203	H-1→LUMO	77	HOMO→L+1	19		
	3	34393	291	0.2010	HOMO->L+1	30	HOMO→L+2	62	H-1→LUMO	4
	4	**34726**	**288**	0.5796	H-1→LUMO	17	HOMO→L+1	48	HOMO→L+2	33
	5	35769	280	0.0011	H-3→LUMO	97				
	6	37426	267	0.0134	H-2→LUMO	29	H-2→L+1	11	HOMO→L+3	55
	7	38369	261	0.0026	H-2→LUMO	69	HOMO→L+3	24	H-1→L+1	4
	8	38808	258	0.0000	HOMO→L+5	98				
	9	40505	247	0.0046	H-4→LUMO	46	H-1→L+2	20	HOMO→L+4	13
	10	**40985**	**244**	0.3004	H-1→L+1	81	H-4→LUMO	9	HOMO→L+3	3
	11	41533	241	0.0206	H-7→LUMO	10	H-1→L+2	42	HOMO→L+4	28
	12	42352	236	0.0030	H-3→L+2	94	H-5→LUMO	3		
	13	42443	236	0.0001	H-5→LUMO	91	H-5→L+1	3	H-3→L+2	3
	14	42771	234	0.0057	H-2→L+1	38	H-1→L+3	21	HOMO→L+3	15
	15	43559	230	0.1024	H-4→LUMO	17	H-1→L+2	12	HOMO→L+4	48

.

Table S10 TD-DFT/B3LYP calculated electronic transitions (absorption maxima λ_{max} in cm^{-1} and nm), oscillator strengths (*f*) and major MO contributors in percent of Co(III) complexes with *E*-1,3-thiazoles and *E*-1,3-selenazoles in DMF solvent.

Compound	No.	λ_{max}		*f*	MO major contributors					
					Transition	%	Transition	%	Transition	%
1-Se	1	15129	661	0.0012	H-1→L+2	54	H-8→L+2	9	H-1→LUMO	9
	2	17165	583	0.0042	H-1→L+1	29	HOMO→LUMO	63		
	3	17406	575	0.0033	H-1→LUMO	36	HOMO→L+1	58		
	4	18368	544	0.0076	H-1→L+1	16	HOMO→L+2	81		
	5	19593	510	0.2780	H-1→L+1	50	HOMO→LUMO	34		
	6	**19719**	**507**	0.3441	H-1→LUMO	52	HOMO→L+1	40		
	7	20551	487	0.0152	H-1→L+3	87	H-1→L+1	2		
	8	20775	481	0.0042	HOMO→L+3	90	H-15→L+3	2		
	9	23134	432	0.0116	H-11→L+2	19	H-8→L+2	17	H-1→L+2	36
	10	24167	414	0.0147	H-17→L+2	13	H-16→L+3	24	H-15→L+2	13
	11	24431	409	0.0033	H-17→L+3	13	H-16→L+2	23	H-15→L+3	13
	12	**27569**	**363**	0.0377	H-2→L+1	13	HOMO→L+4	70	H-1→L+5	8
	13	27607	362	0.0012	H-2→LUMO	69	H-5→L+1	2	HOMO→L+5	9
	14	27801	360	0.0078	H-3→LUMO	14	H-2→L+1	63	HOMO→L+4	16
	15	27822	359	0.0000	H-1→L+4	65	HOMO→L+5	23	H-2→LUMO	7

Table S10 (continued)

Compound	No.	λ_{max}		f	MO major contributors					
					Transition	%	Transition	%	Transition	%
2-Se	1	15192	658	0.0012	H-8→L+2	10	H-1→L+2	49	H-1→LUMO	8
	2	17029	587	0.0016	H-1→L+1	29	HOMO→LUMO	54	HOMO→L+1	10
	3	17222	581	0.0016	H-1→LUMO	44	HOMO→L+1	47		
	4	18390	544	0.0163	H-1→L+1	14	HOMO→L+2	76	H-1→L+2	5
	5	19354	517	0.2784	H-1→L+1	25	HOMO→LUMO	42	HOMO→L+1	15
	6	**19494**	**513**	0.3184	H-1→LUMO	39	H-1→L+1	26	HOMO→L+1	26
	7	20516	487	0.0071	H-1→L+3	78	H-3→L+3	4	HOMO→L+3	9
	8	20855	479	0.0035	HOMO→L+3	80	H-2→L+3	2	H-1→L+3	9
	9	22782	439	0.0093	H-11→L+2	13	H-8→L+2	13	H-1→L+2	34
	10	22972	435	0.0047	H-3→L+1	17	H-2→LUMO	79		
	11	23142	432	0.0034	H-3→LUMO	19	H-2→L+1	66	H-1→L+2	4
	12	24019	416	0.0066	H-17→L+2	16	H-6→L+2	10	H-2→L+2	17
	13	24166	414	0.0027	H-17→L+3	10	H-3→LUMO	33	H-2→L+1	12
	14	24533	408	0.0237	H-3→L+1	80	H-2→LUMO	15		
	15	**27437**	**364**	0.0329	HOMO→L+4	79	H-1→L+5	8	HOMO→L+5	7

Table S10 (continued)

Compound	No.	λ_{max}		*f*	MO major contributors					
					Transition	%	Transition	%	Transition	%
3-Se	1	15535	644	0.0001	H-8→L+2	13	H-1→L+2	61	H-11→L+2	8
	2	17372	576	0.0137	H-1→L+1	27	HOMO→LUMO	71		
	3	17473	572	0.0071	H-1→LUMO	36	HOMO→L+1	62		
	4	18155	551	0.0056	HOMO→L+2	93				
	5	19736	507	0.2654	H-1→L+1	65	HOMO→LUMO	22		
	6	**19871**	**503**	0.3286	H-1→LUMO	58	HOMO→L+1	33		
	7	20726	482	0.0460	HOMO→L+3	83	H-1→L+1	5	HOMO→LUMO	4
	8	20900	478	0.0051	H-1→L+3	89	H-8→L+3	2	H-7→L+3	2
	9	23723	422	0.0029	H-11→L+2	19	H-8→L+2	23	H-1→L+2	32
	10	24390	410	0.0101	H-17→L+3	26	H-16→L+2	16	H-15→L+2	10
	11	24717	405	0.0059	H-17→L+2	24	H-16→L+3	14	H-15→L+3	9
	12	26871	372	0.0016	H-3→L+1	10	H-2→LUMO	57		
	13	26971	371	0.0032	H-3→LUMO	51	H-3→L+1	24		
	14	**27564**	**363**	0.0569	HOMO→L+4	93	H-1→L+5	4		
	15	27825	359	0.0056	H-2→L+1	23	H-2→LUMO	20	HOMO→L+5	33

Table S10 (continued)

Compound	No.	λ_{max}		*f*	MO major contributors					
					Transition	%	Transition	%	Transition	%
1-S	1	15644	639	0.0002	H-9→L+2	24	H-1→L+2	61		
	2	17660	566	0.0179	H-1→L+1	23	HOMO→LUMO	75		
	3	17811	561	0.0088	H-1→LUMO	34	HOMO→L+1	64		
	4	18235	548	0.0044	HOMO→L+2	91	H-1→LUMO	5		
	5	20016	500	0.1941	H-1→L+1	58	HOMO→LUMO	14	HOMO→L+3	21
	6	**20213**	**495**	0.3084	H-1→LUMO	54	HOMO→L+1	32	HOMO→L+2	5
	7	20715	483	0.1014	H-1→L+1	16	HOMO→L+3	69	HOMO→LUMO	9
	8	20867	479	0.0238	H-1→L+3	85	H-9→L+3	4	H-1→LUMO	4
	9	23965	417	0.0031	H-9→L+2	32	H-1→L+2	27	H-11→L+2	8
	10	24481	408	0.0092	H-17→L+3	28	H-16→L+2	15	H-11→L+3	10
	11	24874	402	0.0062	H-17→L+2	21	H-16→L+3	13	H-1→L+2	11
	12	**27871**	**359**	0.0605	HOMO→L+4	94	H-1→L+5	3		
	13	28166	355	0.0173	H-1→L+4	14	HOMO→L+5	84		
	14	28593	350	0.0025	H-3→L+1	13	H-2→LUMO	76	H-5→L+1	3
	15	28715	348	0.0044	H-3→LUMO	38	H-2→L+1	53	H-5→LUMO	5

Table S10 (continued)

Compound	No.	λ_{max}		*f*	MO major contributors					
					Transition	%	Transition	%	Transition	%
2-S	1	15329	652	0.0013	H-9→L+2	20	H-1->L+2	51	H-1→LUMO	8
	2	17397	575	0.0020	H-1→L+1	31	HOMO→LUMO	60	HOMO→L+2	5
	3	17606	568	0.0010	H-1→LUMO	42	HOMO→L+1	49	H-1→L+1	5
	4	18623	537	0.0123	H-1→L+1	15	HOMO→L+2	79		
	5	19728	507	0.2592	H-1→L+1	41	HOMO→LUMO	36	HOMO→L+2	9
	6	**19841**	**504**	0.3235	H-1→LUMO	48	HOMO→L+1	40	H-1→L+1	4
	7	20408	490	0.0209	H-1→L+3	80	H-9→L+3	4	H-3→L+3	4
	8	20771	481	0.0052	HOMO->L+3	86	H-2→L+3	2	H-1→L+3	3
	9	23057	434	0.0126	H-9→L+2	24	H-1→L+2	35	H-23→L+2	8
	10	23266	430	0.0034	H-3→L+1	16	H-2→LUMO	80		
	11	23464	426	0.0028	H-3→LUMO	19	H-2→L+1	69	H-1→L+2	3
	12	24185	413	0.0082	H-17→L+2	17	H-16→L+3	11	H-2→L+2	16
	13	24341	411	0.0004	H-17→L+3	17	H-3→LUMO	16	H-16→L+2	8
	14	24861	402	0.0256	H-3→LUMO	57	H-2→L+1	15	H-17→L+3	5
	15	27750	360	0.0392	HOMO→L+4	78	H-1→L+S	14		

Table S10 (continued)

Compound	No.	λ_{max}		*f*	MO major contributors					
					Transition	%	Transition	%	Transition	%
3-S	1	15659	639	0.0002	H-9→L+2	25	H-1→L+2	61	H-23→L+2	4
	2	17619	568	0.0174	H-1→L+1	24	HOMO->LUMO	75		
	3	17762	563	0.0089	H-1→LUMO	34	HOMO→L+1	65		
	4	18228	549	0.0046	HOMO→L+2	91	H-1→LUMO	5		
	5	19970	501	0.1954	H-1→L+1	58	HOMO→LUMO	14	HOMO→L+3	21
	6	**20167**	**496**	0.3106	H-1→LUMO	55	HOMO→L+1	32	HOMO→L+2	5
	7	20651	484	0.0995	H-1→L+1	15	HOMO→L+3	70	HOMO→LUMO	9
	8	20825	480	0.0193	H-1→L+3	86	H-9→L+3	5	H-1→LUMO	4
	9	23940	418	0.0027	H-9→L+2	33	H-1→L+2	29	H-11→L+2	8
	10	24441	409	0.0091	H-17→L+3	28	H-16→L+2	15	H-11→L+3	10
	11	24794	403	0.0063	H-17→L+2	22	H-16→L+3	13	H-1→L+2	10
	12	26996	370	0.0005	H-3→L+1	26	H-2→LUMO	66	H-2→L+1	6
	13	27041	370	0.0020	H-3→LUMO	56	H-2→L+1	38	H-3→L+1	3
	14	**27790**	**360**	0.0527	HOMO→L+4	89	H-2→L+1	5	H-1→L+5	3
	15	27973	357	0.0066	H-3→L+1	27	H-2→LUMO	16	HOMO→L+5	45

Table S11 Selected highest values of the condensed Fukui functions (f^+ and f^-) for the ligands, considering DFT / DMF / NBO charges according to equations (1 and 2).

Comp. / atom		N_1	N_2	N_3	N_4	C_6	C_8	Se
HLSe[1]	f^+	0.063	0.127	0.004	0.046	0.121	0.053	0.084
	f^-	0.023	–0.006	0.100	0.050	0.082	0.123	0.173
HLSe[2]	f^+	0.064	0.130	0.005	0.047	0.122	0.049	0.081
	f^-	0.018	–0.008	0.069	0.032	0.063	0.127	0.160
HLSe[3]	f^+	0.064	0.129	0.004	0.047	0.121	0.050	0.082
	f^-	0.085	0.122	0.094	0.090	0.197	0.176	0.253

Comp. / atom		N_1	N_2	N_3	N_4	C_6	C_8	S
HLS[1]	f^+	0.064	0.132	0.005	0.047	0.121	0.049	0.073
	f^-	0.025	–0.003	0.106	0.057	0.086	0.139	0.129
HLS[2]	f^+	0.065	0.134	0.006	0.048	0.122	0.046	0.071
	f^-	0.018	–0.007	0.073	0.036	0.066	0.141	0.120
HLS[3]	f^+	0.064	0.134	0.006	0.047	0.122	0.047	0.072
	f^-	0.023	–0.004	0.095	0.050	0.080	0.142	0.127

Table S12 Antifungal activity of investigated compounds tested by the disc-diffusion method (inhibition zone size including disc/mm)

	Inhibition zone diameter[a] (mm)		
Compound	*A. brasiliensis*	*C. albicans*	*S. cerevisiae*
HLSe[1]	10	16	18
HLSe[2]	12	16	22
HLSe[3]	12	22	28
HLS[1]	9	9	10
HLS[2]	10	16	14
HLS[3]	9	12	12
1-Se	16	30	22
2-Se	12	18	14
3-Se	16	20	18
1-S	22	26	22
2-S	n.a.[b]	12	12
3-S	18	24	20
Nystatin	30	32	52

a Including diameter of disc (8 mm);[b] n.a. – not active

REFERENCES

S1 R. Huls and M. Renson, *Bull. des Soc. Chim. Belges*, 1956, **65**, 511–522.

S2 D. R. Goddard, B. D. Lodam, S. O. Ajayi and M. J. Campbell, *J. Chem. Soc. A Inorganic, Phys. Theor.*, 1969, **IV**, 506.

S3 T. R. Todorović, A. Bacchi, D. M. Sladić, N. M. Todorović, T. T. Božić, D. D. Radanović, N. R. Filipović, G. Pelizzi and K. K. Anđelković, *Inorganica Chim. Acta*, 2009, **362**, 3813–3820.

S 4 W. Yi, C. Dubois, S. Yahiaoui, R. Haudecoeur, C. Belle, H. Song, R. Hardré, M. Réglier and A. Boumendjel, *Eur. J. Med. Chem.*, 2011, **46**, 4330–4335.

S 5 H. Elshaflu, S. Bjelogrlić, C. D. Muller, T. R. Todorović, M. Rodić, A. Marinković and N. R. Filipović, *J. Coord. Chem.*, 2016, **69**, 3354–3366.

S 6 CrysAlisPro Software system, Agilent Technologies UK Ltd , Oxford, 2014.

S 7 G. M. Sheldrick, *Acta Crystallogr. Sect. A Found. Adv.*, 2015, **71**, 3–8.

S 8 G. M. Sheldrick, *Acta Crystallogr. Sect. C Struct. Chem.*, 2015, **71**, 3–8.

S 9 C. B. Hübschle, G. M. Sheldrick and B. Dittrich, *J. Appl. Crystallogr.*, 2011, **44**, 1281–1284.

S 10 R. Herbst-Irmer and G. M. Sheldrick, *Acta Crystallogr. Sect. B Struct. Sci.*, 1998, **54**, 443–449.

S 11 A. Altomare, G. Cascarano, C. Giacovazzo and A. Guagliardi, *J. Appl. Crystallogr.*, 1993, **26**, 343–350.

S 12 A. L. Spek, *Acta Crystallogr. Sect. D Biol. Crystallogr.*, 2009, **65**, 148–155.

S 13 H. D. Flack and M. Wörle, *J. Appl. Crystallogr.*, 2013, **46**, 248–251.

S 14 H. D. Flack and G. Bernardinelli, *Acta Crystallogr. Sect. A Found. Crystallogr.*, 1999, **55**,

908–915.

S 15 C. R. Groom and F. H. Allen, *Angew. Chemie Int. Ed.*, 2014, **53**, 662–671.

S 16 M. J. Frisch, G. W. Trucks, H. B. Schlegel, G. E. Scuseria, M. A. Robb, J. R. Cheeseman, G. Scalmani, V. Barone, B. Mennucci, G. A. Petersson, H. Nakatsuji, M. Caricato, X. Li, H. P. Hratchian, A. F. Izmaylov, J. Bloino, G. Zheng, J. L. Sonnenberg, M. Hada, M. Ehara, K. Toyota, R. Fukuda, J. Hasegawa, M. Ishida, T. Nakajima, Y. Honda, O. Kitao, H. Nakai, T. Vreven, J. A. Montgomery Jr., J. E. Peralta, F. Ogliaro, M. Bearpark, J. J. Heyd, E. Brothers, K. N. Kudin, V. N. Staroverov, R. Kobayashi, J. Normand, K. Raghavachari, A. Rendell, J. C. Burant, S. S. Iyengar, J. Tomasi, M. Cossi, N. Rega, J. M. Millam, M. Klene, J. E. Knox, J. B. Cross, V. Bakken, C. Adamo, J. Jaramillo, R. Gomperts, R. E. Stratmann, O. Yazyev, A. J. Austin, R. Cammi, C. Pomelli, J. W. Ochterski, R. L. Martin, K. Morokuma, V. G. Zakrzewski, G. A. Voth, P. Salvador, J. J. Dannenberg, S. Dapprich, A. D. Daniels, Ö. Farkas, J. B. Foresman, J. V. Ortiz, J. Cioslowski and D. J. Fox, 2009.

S 17 A. D. Becke, *J. Chem. Phys.*, 1993, **98**, 5648.

S 18 C. Lee, W. Yang and R. G. Parr, *Phys. Rev. B*, 1988, **37**, 785–789.

S 19 J. P. Perdew, *Phys. Rev. B*, 1986, **33**, 8822–8824.

S 20 A. D. Becke, *Phys. Rev. A*, 1988, **38**, 3098–3100.

S 21 S. H. Vosko, L. Wilk and M. Nusair, *Can. J. Phys.*, 1980, **58**, 1200–1211.

S 22 V. A. Rassolov, J. A. Pople, M. A. Ratner and T. L. Windus, *J. Chem. Phys.*, 1998, **109**, 1223.

S 23 V. A. Rassolov, M. A. Ratner, J. A. Pople, P. C. Redfern and L. A. Curtiss, *J. Comput. Chem.*, 2001, **22**, 976–984.

S 24 P. C. Hariharan and J. A. Pople, *Theor. Chim. Acta*, 1973, **28**, 213–222.

S 25 M. M. Francl, *J. Chem. Phys.*, 1982, **77**, 3654.

S 26 G. Scalmani and M. J. Frisch, *J. Chem. Phys.*, 2010, **132**, 114110.

S 27 N. T. Abdel Ghani and A. M. Mansour, *J. Mol. Struct.*, 2011, **991**, 108–126.

S 28 L. Miao, Y. Yao, F. Yang, Z. Wang, W. Li and J. Hu, *J. Mol. Struct. THEOCHEM*, 2008, **865**, 79–87.

S 29 E. S. Böes, P. R. Livotto and H. Stassen, *Chem. Phys.*, 2006, **331**, 142–158.

S 30 Y. Li and J. N. S. Evans, *J. Am. Chem. Soc.*, 1995, **117**, 7756–7759.

S 31 R. G. Parr and W. Yang, *Functional Theory of Atoms and Molecules*, Oxford University Press, New York, 1989.

S 32 E. D. Glendening, A. E. Reed, J. E. Carpenter and F. Weinhold, NBO Version 3.1.

S 33 C. Perez, M. Pauli and P. Bazerque, *Acta Biol. Med. Exp.*, 1990, **15**, 113–115.

S 34 R. S. Nicholson, *Anal. Chem.*, 1965, **37**, 1351–1355.

S35 M. V. de O. Cardoso, L. R. P. de Siqueira, E. B. da Silva, L. B. Costa, M. Z. Hernandes, M. M. Rabello, R. S. Ferreira, L. F. da Cruz, D. R. Magalhães Moreira, V. R. A. Pereira, M. C. A. B. de Castro, P. V. Bernhardt and A. C. L. Leite, *Eur. J. Med. Chem.*, 2014, **86**, 48–59.